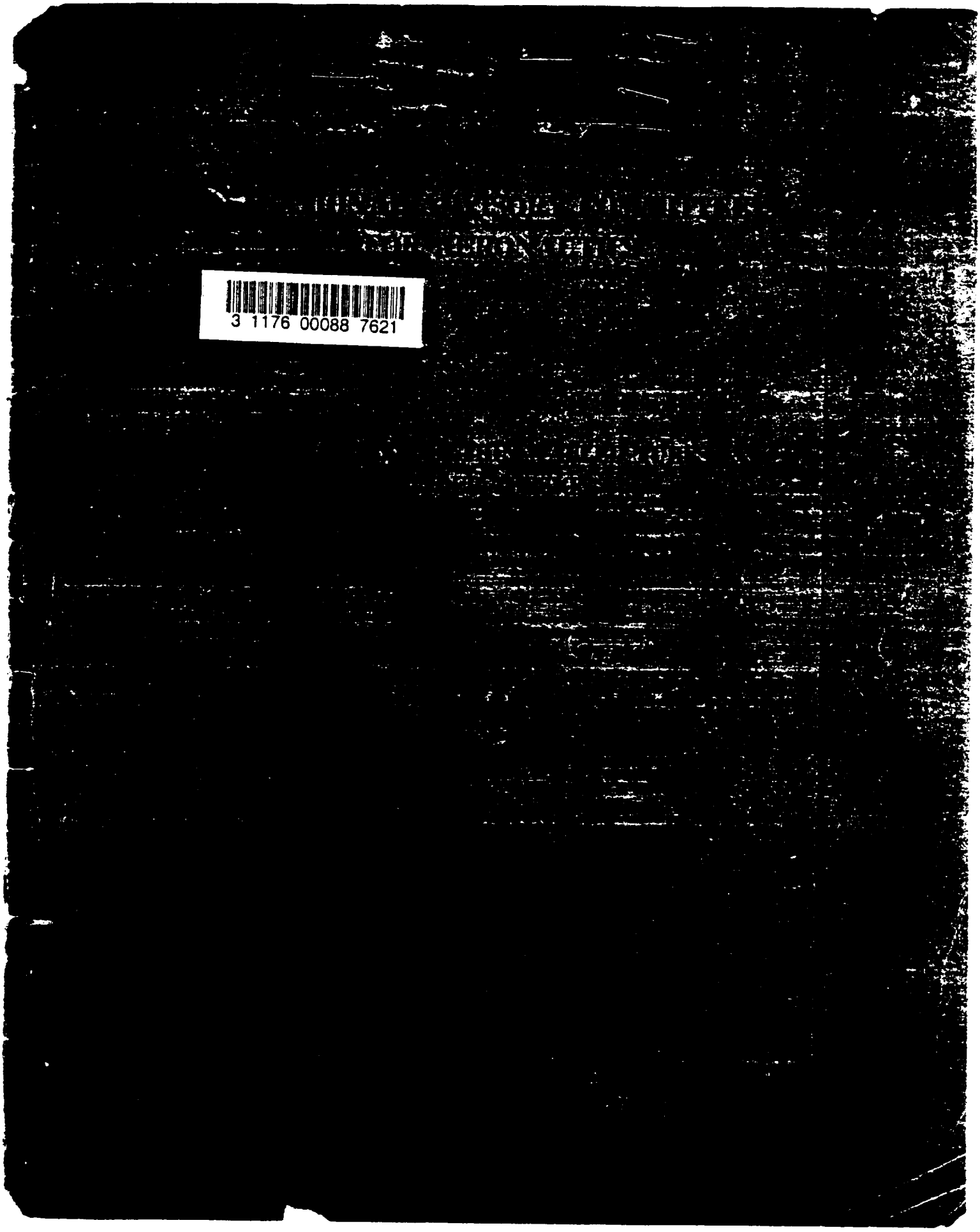

[redacted]

REPORT No. 479

STABILITY OF THIN-WALLED TUBES UNDER TORSION

By L. H. DONNELL
California Institute of Technology

12402—33——1

NATIONAL ADVISORY COMMITTEE FOR AERONAUTICS

NAVY BUILDING, WASHINGTON, D.C.

(An independent Government establishment, created by act of Congress approved March 3, 1915, for the supervision and direction of the scientific study of the problems of flight. Its membership was increased to 15 by act approved March 2, 1929 (Public, No. 908, 70th Congress). It consists of members who are appointed by the President, all of whom serve as such without compensation.)

JOSEPH S. AMES, Ph.D., *Chairman*,
President, Johns Hopkins University, Baltimore, Md.
DAVID W. TAYLOR, D.Eng., *Vice Chairman*,
Washington, D.C.
CHARLES G. ABBOT, Sc.D.,
Secretary, Smithsonian Institution, Washington, D.C.
LYMAN J. BRIGGS, Ph.D.,
Director, Bureau of Standards, Washington, D.C.
ARTHUR B. COOK, Captain, United States Navy,
Assistant Chief, Bureau of Aeronautics, Navy Department, Washington, D.C.
WILLIAM F. DURAND, Ph.D.,
Professor Emeritus of Mechanical Engineering, Stanford University, California.
BENJAMIN D. FOULOIS, Major General, United States Army,
Chief of Air Corps, War Department, Washington, D.C.
HARRY F. GUGGENHEIM, M.A.,
Port Washington, Long Island, New York.
ERNEST J. KING, Rear Admiral, United States Navy,
Chief, Bureau of Aeronautics, Navy Department, Washington, D.C.
CHARLES A. LINDBERGH, LL.D.,
New York City.
WILLIAM P. MACCRACKEN, Jr., Ph.B.,
Washington, D.C.
CHARLES F. MARVIN, Sc.D.,
Chief, United States Weather Bureau, Washington, D.C.
HENRY C. PRATT, Brigadier General, United States Army,
Chief, Matériel Division, Air Coprs, Wright Field, Dayton, Ohio.
EDWARD P. WARNER, M.S.,
Editor "Aviation," New York City.
ORVILLE WRIGHT, Sc.D.,
Dayton, Ohio.

GEORGE W. LEWIS, *Director of Aeronautical Research.*
JOHN F. VICTORY, *Secretary.*
HENRY J. E. REID, *Engineer in Charge, Langley Memorial Aeronautical Laboratory, Langley Field, Va.*
JOHN J. IDE, *Technical Assistant in Europe, Paris, France.*

EXECUTIVE COMMITTEE

JOSEPH S. AMES, *Chairman.*
DAVID W. TAYLOR, *Vice Chairman.*

CHARLES G. ABBOT.
LYMAN J. BRIGGS.
ARTHUR B. COOK.
BENJAMIN D. FOULOIS.
ERNEST J. KING.
CHARLES A. LINDBERGH.
WILLIAM P. MACCRACKEN, Jr.
CHARLES F. MARVIN.
HENRY C. PRATT.
EDWARD P. WARNER.
ORVILLE WRIGHT.

JOHN F. VICTORY, *Secretary.*

REPORT No. 479

STABILITY OF THIN-WALLED TUBES UNDER TORSION

By L. H. DONNELL

SUMMARY

In this paper a theoretical solution is developed for the torsion on a round thin-walled tube for which the walls become unstable. The results of this theory are given by a few simple formulas and curves which cover all cases. The differential equations of equilibrium are derived in a simpler form than previously found, it being shown that many items can be neglected. The solution obtained is "exact" for the two extreme cases when the diameter-length ratio is zero and infinite, and is a good approximation for intermediate cases. The theory is compared with all available experiments, including about 50 tests made by the author. The experimental-failure torque is always smaller than the theoretical-buckling torque, averaging about 75 percent of it, with a minimum of 60 percent. As the form of the deflection checks closely with that predicted by theory and the experiments cover a great range of shapes and materials, this discrepancy can reasonably be ascribed largely to initial eccentricities in actual tubes.

SYMBOLS

l, t, r, d, length, thickness of wall, and mean radius and diameter of the tube, respectively.

E, μ, Young's modulus, and Poisson's ratio (0.3 for engineering metals).

S, critical shear stress (equals the critical torque times $\frac{2}{\pi d^2 t}$)

n, number of circumferential waves in buckling deformation.

θ, angle of waves with the axis, measured near the middle of the tube.

x, s, longitudinal and circumferential coordinates, measured axially from the normal section at the middle of the tube, and circumferentially from some genetrix, figure 13.

u, v, w, longitudinal, circumferential, and radial components of the displacement during buckling, taken as positive in the x, s, and outward directions, figure 13.

ϵ_x, ϵ_s, ϵ_{xs}, κ_x, κ_s, κ_{xs}, linear strains in the x and s directions and the shearing strain, and the changes in curvature in the x and s directions and the unit twist, all due to the buckling displacement.

T_x, T_s, T_{xs}, T_{xs}', N_x, N_s, G_x, G_s, G_{xs}, G_{xs}', resultant normal and shear forces, and resultant bending and twisting moments, due to the buckling displacement, all reckoned per unit length of section, as shown in figure 14.

λ_1, λ_2, $-\lambda_m$, numbers relating to the axial length of buckling waves.

$\lambda_1 = a+b$, $\lambda_2 = a-b$, $\lambda_3 = -a+ic$, $\lambda_4 = -a-ic$, where a, b, c are real numbers.

U_m, V_m, W_m are real numbers used in the expressions (13) for u, v, and w.

$\nabla^2 = \frac{\partial^2}{\partial x^2} + \frac{\partial^2}{\partial s^2}$, ∇^4 signifies application of ∇^2 twice, etc.

$$A = (1-\mu^2)\frac{S}{E}\frac{l^2}{t^2},\quad B = \sqrt{1-\mu^2}\,\frac{S}{E}\frac{l}{t}$$

$$H = \sqrt{1-\mu^2}\,\frac{l^2}{td},\quad J = \frac{1}{\sqrt{1-\mu^2}}\frac{l^2 t}{d^3},\quad k = n\frac{l}{d}$$

All equations given in the paper are dimensionally correct, so any consistent units of distance and force may be used.

RESULTS

According to the theory developed in this paper, the torsional shear stress at which buckling occurs in short and moderately long tubes is given by the full lines in figure 1, or is very nearly expressed by the formulas

$$\begin{aligned} A &= 4.6 + \sqrt{7.8 + 1.67H^{3/2}} \text{ (clamped edges, } J < 7.8) \\ A &= 2.8 + \sqrt{2.6 + 1.40H^{3/2}} \text{ (hinged edges, } J < 5.5) \end{aligned} \quad (1)$$

It is assumed that all components of displacement are prevented at end cross sections of the tube, and that "clamped" edges are held perpendicular to these cross sections while "hinged" edges are free to change their angle with the cross sections. It is found to be immaterial whether or not the ends of the tube are free to move as a whole.

For very long slender tubes the number of circumferential waves, n, is small, and there is a slight deviation from the above laws, as the number of waves changes from one whole number to the next. In figure 2 the straight lines de represent the above laws, while the irregular lines represent the more exact law. When J exceeds a certain value, n remains always 2 (at least for any tubes of practical proportions). For large values of J the critical stress for both end conditions

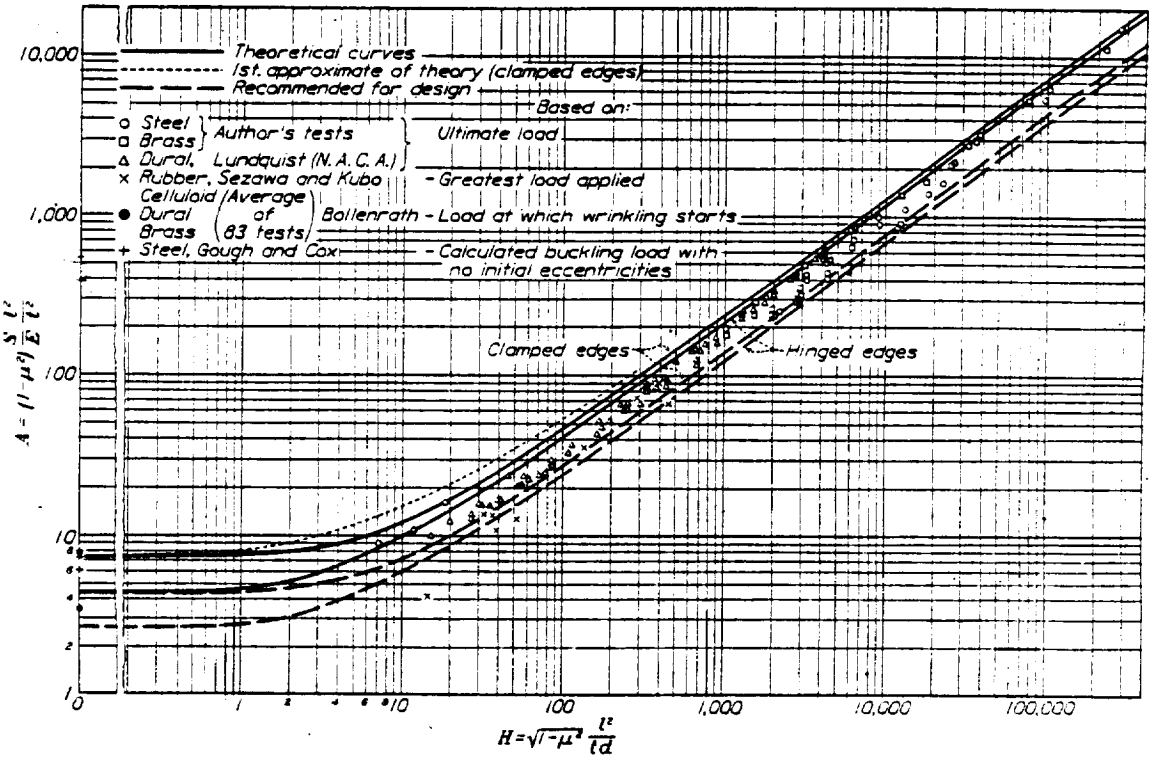

FIGURE 1.—Critical torsion stress for short and medium length tubes.

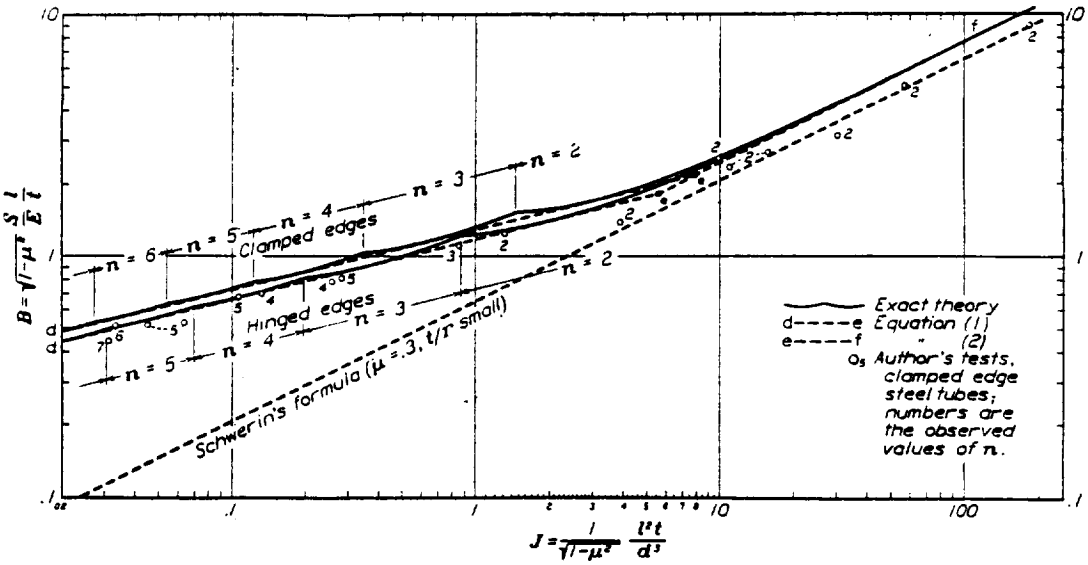

FIGURE 2.—Critical torsion stress for long slender tubes.

is given very nearly by the straight line eef, whose equation is

$$B = 0.77\sqrt{J} \qquad (2)$$

For practical purposes equation (1) may be used when J is less than 7.8 for clamped edges, or 5.5 for hinged edges, as indicated in (1), while (2) is used when J exceeds these values.

If buckling takes place all around the tube, n must naturally be a whole number, and its value may be taken as the whole number nearest to the value found from figure 3. In many tests, especially when n is large, buckling takes place over only part of the tube. In such a case n is taken as the circumference divided by the average width of the waves, and it therefore need not be a whole number.

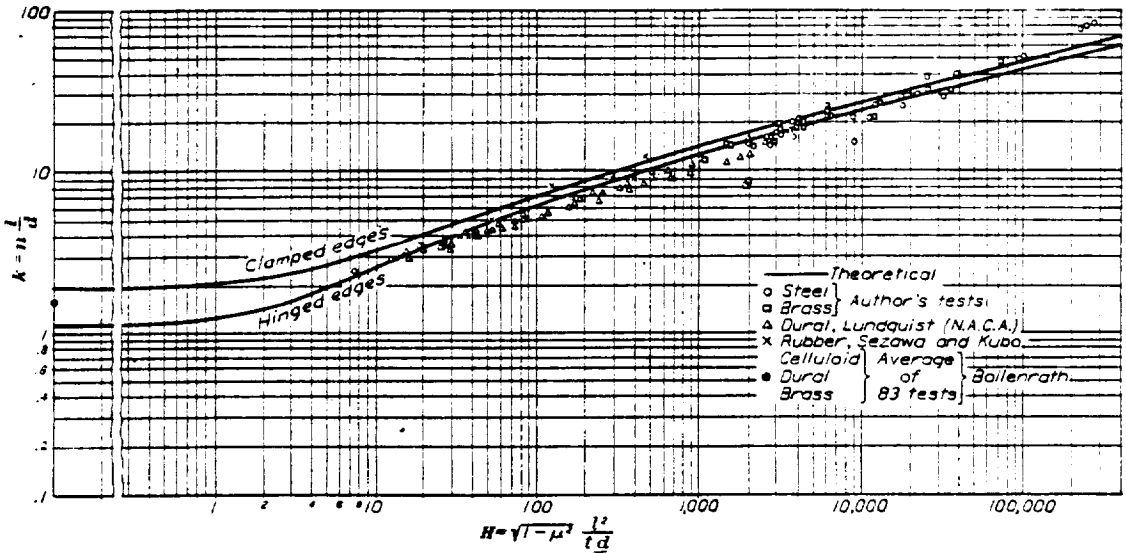

FIGURE 3.—The number of circumferential waves for short and medium length tubes.

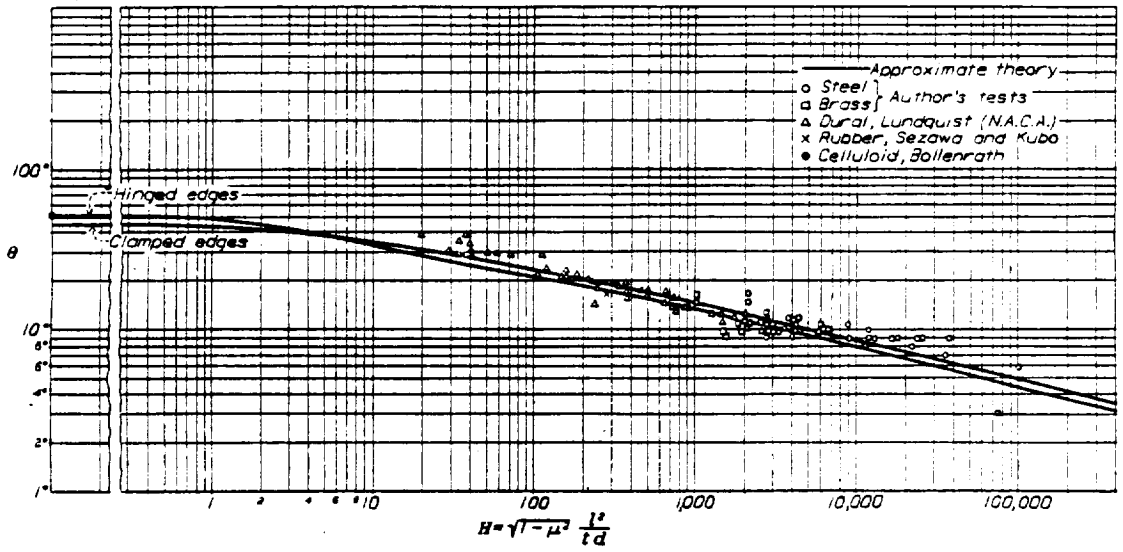

FIGURE 4.—The angle of the waves with respect to the cylinder axis for short and medium length tubes.

The buckling deformation consists of a number of circumferential waves which spiral around the tube from one end to the other, as shown by the photographs of actual specimens (fig. 6). The theoretical number of circumferential waves, n, is indicated in figure 2 for long slender tubes. For short or moderately long tubes the theoretical value of n is given by the curves of figure 3.

The theoretical angle of the waves with the axial direction, near the middle of the tube, θ, is given in figure 4 for short and moderately long tubes. For long slender tubes it may be taken as

$$\theta = \frac{235d}{nl} \text{ (clamped edges)} \qquad (3)$$

$$\theta = \frac{184d}{nl} \text{ (hinged edges)}$$

in degrees, where n is as given in figure 2.

To check the above theoretical results, the author has made more than 50 tests; in addition, the results of many other experiments have been published by the N.A.C.A. (reference 1) and others. All the available test results have been plotted on figures 1, 2, 3, and 4. All the tests were made with clamped edges. Comparing the experimental results with the theoretical curves for clamped edges, it will be seen that all tests give values for the failure stress somewhat lower than the values for critical stress predicted by theory. The experimental values average about 75 percent of the theoretical, with a minimum for metal tubes of about 60 percent of the theoretical.

These relations hold over an enormous range of sizes, proportions, and materials. The form of the buckling deflection, as measured by the number and angle of the waves, checks closely with that predicted by theory. It is therefore reasonable to suppose that the discrepancy between the theoretical and experimental values of failure stress is due chiefly to unavoidable defects in actual tubes. Some of the discrepancy is undoubtedly due to the fact that a true clamped edge is impossible to attain in practice. But it is probable that most of it can be ascribed to initial eccentricities; that is, departures from a true cylindrical form, always present in actual tubes. Among the tests made on long flat strips in shear (which is con sidered the limiting case of a tube under torsion when $H=0$), those made by Bollenrath (reference 2) record the stress at which wrinkling *began*, and these stresses average less than half the theoretical, as shown in figure 1. Similar results were obtained by Gough and Cox (reference 3), but these experimenters took measurements of the buckling deflections at various loads and with this data were able to calculate, by a method developed by Southwell (reference 4), the probable load at which the strips would have buckled if there had been no eccentricities. These calculated values check the theoretical values very well, as shown in figure 1. It seems likely that most of the discrepancies in the tests on tubes could be explained in the same manner if similar data were available.

By multiplying the right-hand sides of equations (1) and (2) by the factor 0.75 or 0.60, we obtain, respectively, expressions for the *average* and *minimum* resistance to buckling to be expected from an actual tube. The following equations are obtained by multiplying the right-hand sides of equations (1) by 0.60 and taking $\mu=0.3$:

$$S=E\left(\frac{t}{l}\right)^2\left[3.0+\sqrt{3.5+.68\frac{l^3}{(td)^{\frac{1}{2}}}}\right] \text{ (clamped edges)}$$
$$S=E\left(\frac{t}{l}\right)^2\left[1.8+\sqrt{1.2+.57\frac{l^3}{(td)^{\frac{1}{2}}}}\right] \text{ (hinged edges)} \quad (4)$$

These formulas cover all present-day applications and are recommended for design purposes. Being based on the *minimum* results from all available tests on metal tubes, more than 120 tests, they should give values which are always on the safe side. They are represented graphically by the broken lines in figure 1.

The case of hinged edges has an application, for example, in the case of a circular monocoque fuselage, without longitudinal stiffeners and with circumferential stiffeners or rings of an open cross section, with small stiffness against twist. The portions of the covering between rings are very nearly in the condition of tubes with hinged edges, as the rings, while stiff against linear movements, give little resistance to rotation of the edges. In such a case there is little interference between adjacent sections of the covering in buckling, as where one section buckles outward the next section can buckle in.

HISTORY OF PROBLEM

In 1883 Greenhill obtained a solution for the stability under torsion of a long solid shaft (reference 10). This solution applies also to hollow shafts or tubes, representing a solution for the case $n=1$. It will be shown later that this solution can be obtained in a much simpler way, and that it actually has little practical importance.

The first paper on thin walled tubes under torsion seems to have been written by Schwerin (reference 5) in 1924. He develops the following formula for the critical stress of tubes in torsion

$$S=0.248E\left(\frac{t}{r}\right)^{\frac{3}{2}}\left(1+0.45\frac{t}{r}\right)$$

The values found in experiments are mostly much higher than those given by this formula. For the shorter tubes the test results are 30, or more, times the formula value; for longer tubes the discrepancy decreases. The value in the final parenthesis in the above formula is practically unity, as with available materials t/r must be very small if failure by buckling occurs before failure of the material. If this value is taken as unity, Schwerin's equation checks equation (2), except for a difference of about 16 percent in the coefficient, as shown in figure 2. Schwerin obtained his result from a solution of differential equations of equilibrium, by neglecting all end constraints and assuming that $n=2$. Equation (2) is also for the case $n=2$, and as it holds for both clamped and hinged edges, it is evident that end conditions are unimportant in the range to which it applies. From this check and from the check with experiments, it is evident that Schwerin's equation is an at least approximately correct solution for *very long slender tubes*, that is, for the range, say, when $J>6$.

The above equation is the only part of Schwerin's paper which is commonly quoted. However Schwerin also discussed in this paper the cases where n has other values than 2. He checked Greenhill's result

for the case $n=1$, and showed how individual results could be obtained with other values of n, and with a consideration of end conditions. He calculated the relation between the buckling stress and r/l for several values of n and for several values of t/r, with the end conditions $x=\pm l/2$: $w=0$. These calculations give good checks with the theory and experiments found by the author for more specific end conditions. However Schwerin failed to develop any way of simplifying his results, except for the case discussed above, and he did not carry them far enough to be of practical value to users of short or moderately long thin-walled tubes.

In the same year (1924) a solution was published by Southwell and Skan (reference 6) for the critical shearing stress on a flat strip of infinite length. This case may be considered to be the limiting case for a tube under torsion, when the ratio of length to diameter becomes zero. As the theory of the present paper is "exact" for this extreme case, it concides with the Southwell and Skan theory when l/d is set equal to zero. The existence of this solution for a limiting case was naturally of great help to the author in developing a general theory of torsional stability, and many valuable suggestions were taken from the ingenious methods of solution used by these writers.

In 1931 a paper on the buckling of tubes under torsion was published by Sezawa and Kubo (reference 7). In this a general theory is developed and worked out for a number of cases, and nine very complete tests on rubber models are reported. The results of this theory are not in agreement with experimental results. The experiments on rubber models cited in the paper happen to be in a range where the discrepancy is not so great, the ratio between the critical stress found by experiment and that predicted by the theory being from 0.5 to 3. However, for most of the available experiments on metal cylinders, this ratio is much higher—as much as 50 or more in many cases. The differential equations of equilibrium on which the solution is based seem to be incorrect, the very important term T_2/a (using the paper's symbols) having apparently been omitted from the third equation.

The results of the experiments described by Sezawa and Kubo are reasonably consistent with the results of other experiments and the theory of the present report (see fig. 1), and certainly as consistent as could be expected when it is considered that a material was used which many experimenters consider unsuitable for quantitative work. The check is excellent in respect to n and θ, which do not depend on E (figs. 3 and 4). In reference 7 very complete data are given on the shape taken by the specimens at all stages of the loading, from the unloaded condition to the critical load. This data affords a very interesting picture of the way in which the deflection, starting from the initial unevenesses, changes to the final buckling form. A method of studying this question theoretically has been suggested by the present author (reference 8), and applied to the case of simple struts. This question is doubtless more of academic than of practical interest.

In 1932, the National Advisory Committee for Aeronautics published the results of an extensive series of tests by Lundquist (reference 1) on the strength in torsion of thin-walled duralumin tubes. No theoretical analysis was attempted. These tests, together with the tests made by the author, constitute the bulk of the experimental evidence cited in the present paper.

In 1932, also, a theoretical paper was published by Sanden and Tölke (reference 11) on the stability of thin cylinders, the case of torsion being considered among others. These authors used very complete and therefore complex equations of equilibrium, but they carried their work on torsion no farther than Schwerin. It is very interesting to note that their equation 130b, for the case $n=2$, is exactly the same as equation (2) of the present paper, which was obtained independently with very much simplified equilibrium equations.

The experimental results of Bollenrath (reference 2), published in 1929, and of Gough and Cox (reference 3), published in 1932, on narrow flat strips in shear, have already been discussed.

THE TESTS AND DESCRIPTION OF SPECIAL TESTING APPARATUS

The author's tests were performed at the Guggenheim Aeronautical Laboratory of the California Institute of Technology. With one exception the specimens were of small size, from $\frac{5}{16}$ inch to 6 inches diameter, and made of steel and brass "shim stock" from 0.002 inch to 0.006 inch thick. Such sizes were selected because of the great ease and cheapness of construction and testing. The exception mentioned was very much larger (27 inch diameter); all the N.A.C.A. tests (reference 1) were on specimens 15 inches and 30 inches in diameter. Comparison of the results indicates that there is no great disadvantage or danger in using such small specimens. In all tests the proportions were such that the stresses were always well below the elastic limit.

The material was carefully rolled around rods of proper diameter to give it approximately the desired curvature, the longitudinal seams were soldered, and the tubes were then soldered to heavy end pieces. Jigs were used to hold the material in a true cylindrical form and prevent local waving while these soldering operations were performed. The specimens having the smallest t/d ratios showed some initial waves, due chiefly to lack of flatness in the stock from which they were made; but in the specimens with larger t/d ratio no departure from true cylindrical form could be detected by the eye or fingers.

The longitudinal seams were lapped about $\frac{1}{16}$ inch and were formed with as little solder as possible.

There is no theoretical reason why such a seam should have an appreciable effect in this type of loading. Buckling deflections seemed to occur across seams as freely as anywhere, so the stiffening effect of the double thickness at the seam was probably negligible in all cases except possibly for the few tubes which were only $\frac{5}{16}$ inch in diameter. For these tubes an attempt was made to correct as much as possible for this stiffening effect by taking the thickness as the total cross-sectional area of the tube wall divided by the circumference.

The end conditions of the tubes were as shown in figure 5. The medium length tubes (6 to 30 inches long) were soldered to heavy end plates as shown at (a). Heat was applied only to the end plates and care

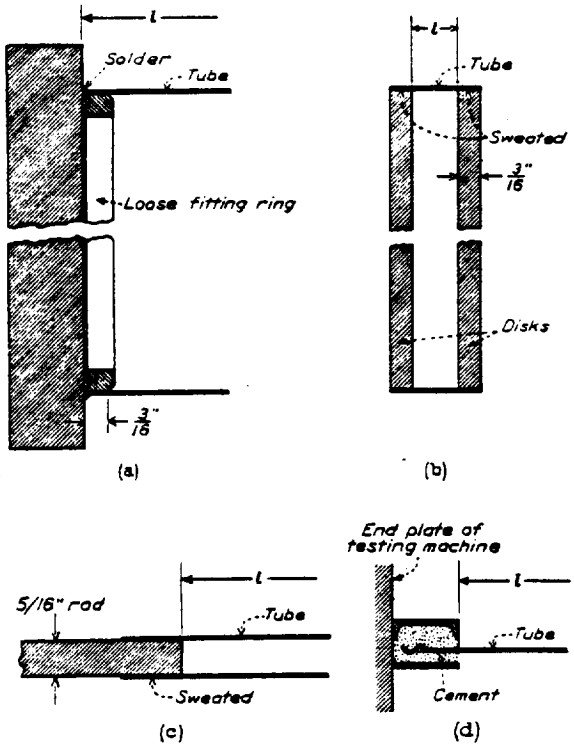

FIGURE 5.—Edge conditions of test specimens.

was taken to heat them symmetrically to avoid producing initial strains in the tube. The loose ring shown in the figure fitted the tube just closely enough to keep the tube cylindrical during the soldering. As there was always a certain amount of clearance between the ring and the tube wall and buckling deflections were not appreciable at a distance from the end many times the width of the ring (see fig. 6), the effect of the ring on the end conditions was neglected and the distance between the end plates was taken as the length of the tubes.

Several extremely short specimens were made, to test the theory at small values of H. As both theory and common sense indicate the greater importance of end conditions for such a case, great care was taken to obtain definite end conditions. One side of a strip of material $\frac{1}{8}$ inch wider than the desired tube length was tinned on one side with a very thin coating of solder. The mechanical properties of similar sheet material were measured after tinning and found to be the same as before tinning, as nearly as could be determined. Two disks were turned the size of the desired tube, their edges were thinly tinned, the tinned strip was tightly clamped around them as shown in figure 5 (b), and the whole heated so as to sweat the tube to the disks. Examination after testing showed a perfect joint between the tube and the disks right up to the edges of the disks.

The $\frac{5}{16}$-inch-diameter tubes were merely sweated over the end of a steel rod as shown in figure 5 (c). The 27-inch tube had bolted joints, and its ends were embedded in concrete, held between steel hoops, as shown at (d). The hoops were clamped to the heavy end plates of the testing machine, and the length of the tube was measured as shown.

The medium and very short specimens were tested on the special testing machine shown in figure 6.

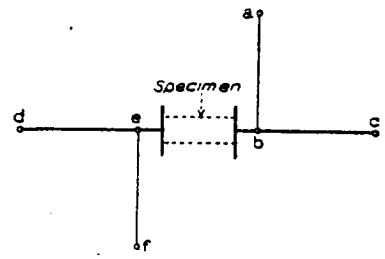

FIGURE 7.—Diagrammatic top view of torsion-bending-compression testing machine.

This machine is capable of testing specimens in torsion, uniform or varying bending, and axial compression, separately or in any combination. The three types of load are applied by three conveniently located cranks, and the load application is extremely smooth. The load is read directly in inch-pounds and pounds, on three dial gages. These dial gages measure the deflections of cantilever springs which are designed in such a way as to eliminate practically all hysteresis and are artificially aged. Provision is made for adjusting the position of the dial gages lengthwise of the springs so that, in calibrating, a position can be found at which they read the loads directly.

The principle of the machine is shown by the diagrammatic top view (fig. 7). The specimen is attached to two L-shaped members abc and def which are balanced on practically frictionless universal joints at b and e. The ends of the specimen are therefore free to rotate in any direction. When axial loads are used they are applied through these universal joints and this insures a definite line of action of the load. The specimen is subjected to bending by applying downward forces at d and c; these forces are applied through

wires which extend down to a cross bar dc under the specimen. A crank is used to press down on a fulcrum mounted on the bar dc; the crank and fulcrum are movable along the length of dc, and in this way the ratio between the forces at d and c, and therefore the bending moments at the two ends of the specimen, can be varied at will. Torsion is applied to the specimen by pulling down on f through a wire, by means of a crank; the point a is prevented from vertical (but not from horizontal) motion by vertical wires. Axial load is applied by moving point b to the left with a crank; e is mounted on one of the cantilever springs and thus the axial load is measured. The arms bc and ab are in themselves cantilever springs and their deflection measures the bending and torsion moments respectively. The dial gages which measure the deflections of the springs are mounted on unstressed arms.

The universal joints at b and e are of the type shown in figure 8*a*, consisting only of a spherical cup, a central ball and six loose balls (the weight of the member abc or def is sufficient to keep the balls in position). This joint takes loads in two directions, allows rotation in any direction with almost no friction, and is extremely cheap and satisfactory. The whole testing machine is built of structural shapes, assembled largely by welding, with a minimum of machining. It cost very little to build and has proved very satisfactory and convenient to use.

The 27-inch diameter specimen was tested on a special testing machine similar to the one just described but much larger (fig. 9). No provision for axial loading is made on this machine, and the loads are measured by the lateral deflection of tension members that are initially bent, which permits the measurement of very large forces with a light measuring device. This machine takes specimens up to 3 feet in diameter and 15 feet in length, and has a capacity of 500,000 inch-pounds in bending and in torsion.

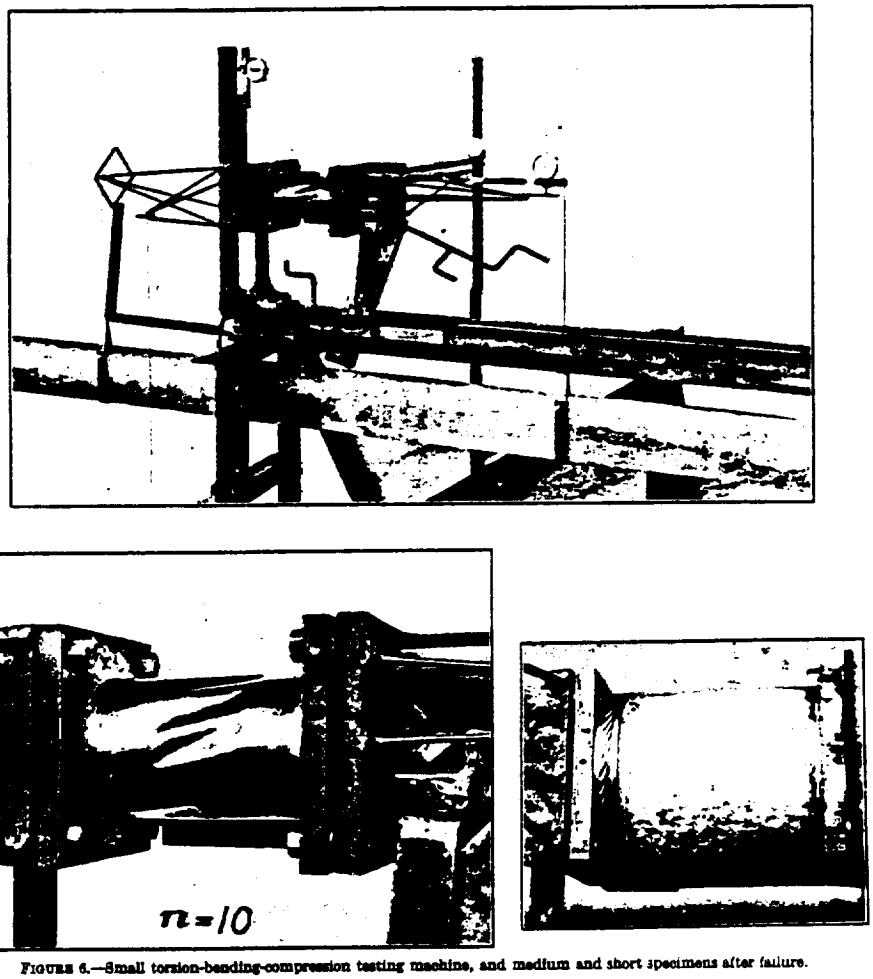

FIGURE 6.—Small torsion-bending-compression testing machine, and medium and short specimens after failure.

The $\frac{1}{16}$-inch diameter specimens, used to test the theory for long slender tubes, were loaded as shown in figure 10. T-shaped pieces were attached to the ends of the specimen. These were balanced on a knife-edge

wires which extend down to a cross bar dc under the specimen. A crank is used to press down on a fulcrum mounted on the bar dc; the crank and fulcrum are movable along the length of dc, and in this way the ratio between the forces at d and c, and therefore the bending moments at the two ends of the specimen, can be varied at will. Torsion is applied to the specimen by pulling down on f through a wire, by means of a crank; the point a is prevented from vertical (but not from horizontal) motion by vertical wires. Axial load is applied by moving point b to the left with a crank; e is mounted on one of the cantilever springs and thus the axial load is measured. The arms bc and ab are in themselves cantilever springs and their deflection measures the bending and torsion moments respectively. The dial gages which measure the deflections of the springs are mounted on unstressed arms.

The universal joints at b and e are of the type shown in figure 8*a*, consisting only of a spherical cup, a central ball and six loose balls (the weight of the member abc or def is sufficient to keep the balls in position). This joint takes loads in two directions, allows rotation in any direction with almost no friction, and is extremely cheap and satisfactory. The whole testing machine is built of structural shapes, assembled largely by welding, with a minimum of machining. It cost very little to build and has proved very satisfactory and convenient to use.

The 27-inch diameter specimen was tested on a special testing machine similar to the one just described but much larger (fig. 9). No provision for axial loading is made on this machine, and the loads are measured by the lateral deflection of tension members that are initially bent, which permits the measurement of very large forces with a light measuring device. This machine takes specimens up to 3 feet in diameter and 15 feet in length, and has a capacity of 500,000 inch-pounds in bending and in torsion.

The $\frac{1}{16}$-inch diameter specimens, used to test the theory for long slender tubes, were loaded as shown in figure 10. T-shaped pieces were attached to the ends of the specimen. These were balanced on a knife-edge

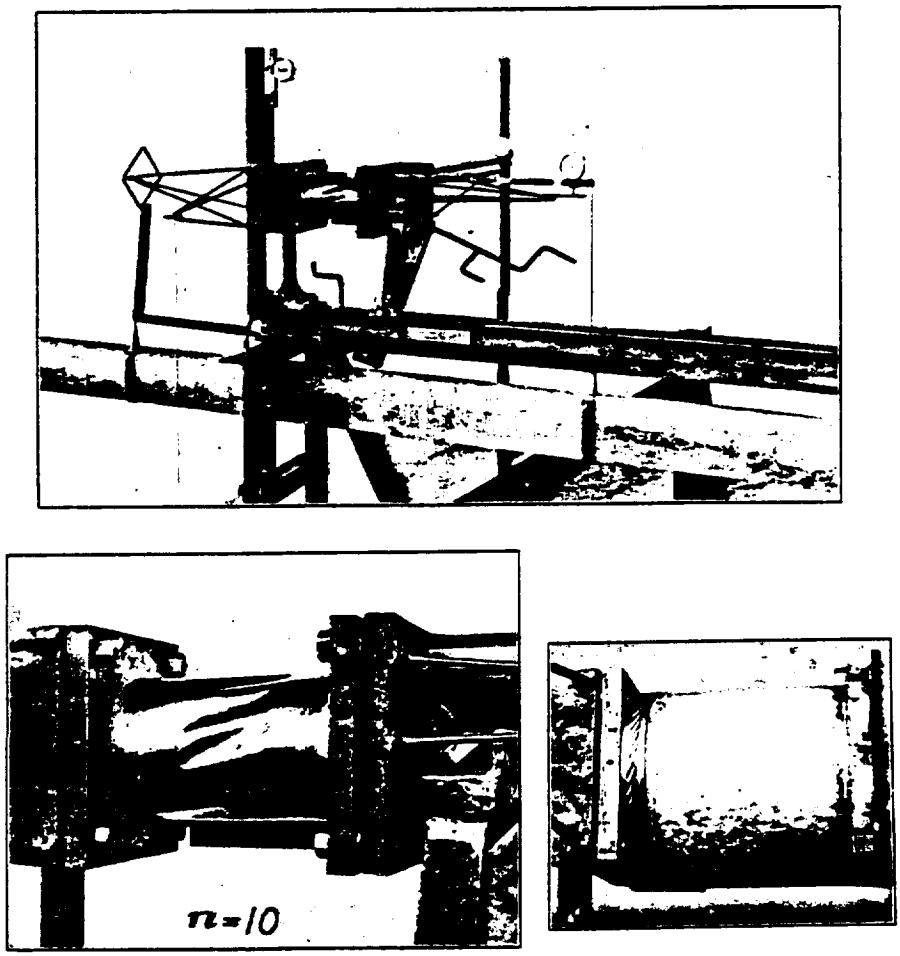

FIGURE 6.—Small torsion-bending-compression testing machine, and medium and short specimens after failure.

at one end and on a loose vertical strip at the other, so that the ends of the specimen were free to rotate in any direction or to approach each other (as was also the case with the testing machines previously described). The long arm of the T at one end was held down with a string, while weights were applied to the other until buckling occurred, as shown in the figure.

The wall thickness of the specimens being so small, it was necessary to measure it with much more than common accuracy. The instrument shown in figure 11 which surrounds the anvil. Such provisions are necessary to measure the thickness of thin material accurately. The sheet must also be very clean, as particles of dust or films of dirt causes appreciable errors; it was found advisable to wet the sheet with alcohol during the measuring. In spite of such precautions, the errors in the measurement of t and in the variation in the thickness at different parts of the sheet undoubtedly cause a large part of the scatter in the final results. The variation in thickness over a tube was usually

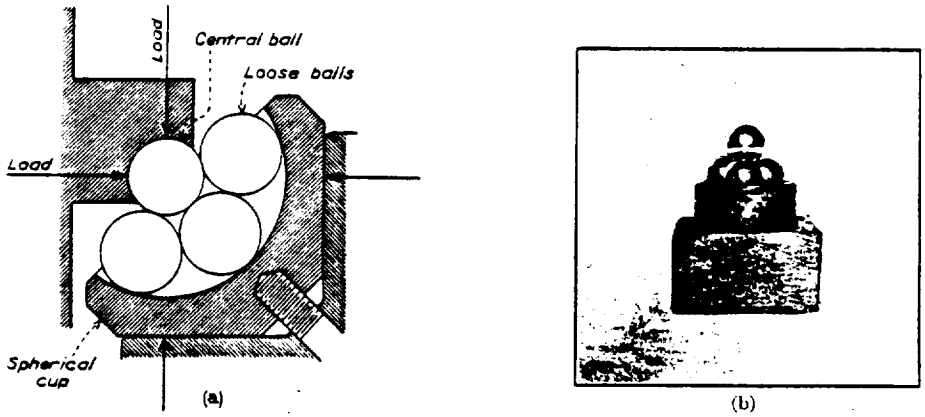

FIGURE 8.—Ball universal joints used in the testing machines (b, type used on large machine for vertical loads only, 1 in. balls, capacity 5,000 lb.)

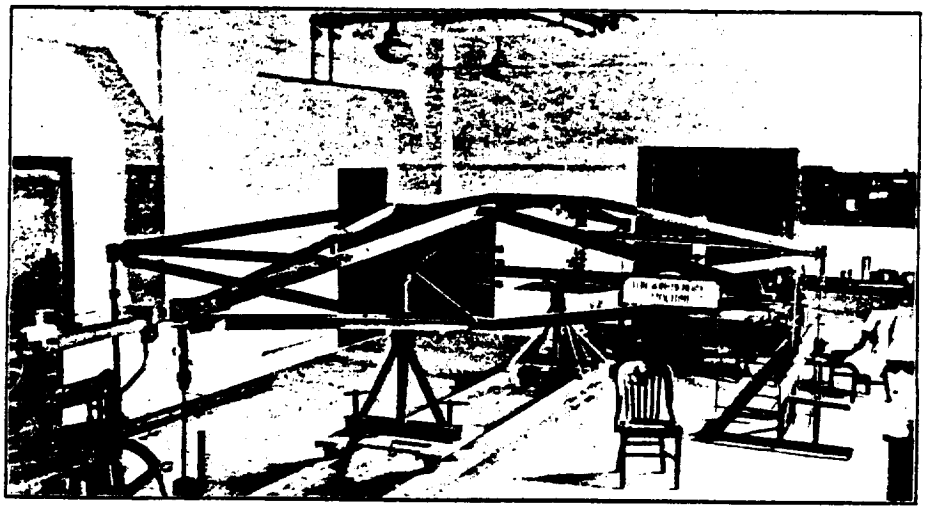

FIGURE 9.—Corner of aeronautical-structures laboratory at California Institute of Technology, showing 500,000 in.-lb. torsion-bending testing machine.

was therefore constructed; it is 10 times as sensitive as an ordinary micrometer and proved to be much more accurate and convenient. It consists of a vertically mounted dial gage reading in 0.01 mm (.00039 in.) and having an extra strong spring and a very smooth contact point, so that a sheet can be moved under it smoothly. Directly under the contact point of the gage an adjustable rounded anvil projects slightly above the flat bedplate of the machine. The sheet is pressed down on this anvil by a spring-actuated ring about 5 percent. As torsion failure occurs over most of the tube at once, the average thickness was recorded.

The modulus of elasticity of the material of the tubes was measured by the special testing machines shown in figure 12. The one shown at (a) is a tensile machine with a capacity of 130 pounds. The force is measured by the calibrated spring at the top, the dial reading directly in tenths of a pound. The specimens used are plain straight strips 1 inch wide. They are clamped in ordinary straight jaws lined with emery cloth; such

thin materials are easily held by friction alone. As the machine is frequently used to determine elastic limits, provision is made to insure perfectly central loading. The extensometer shown involves a detachable Huggenberger instrument mounted on a special frame, with provisions for clamping to thin sheet and

It was feared that the physical properties of such thin, highly cold-worked material might vary along the thickness. In order to test this, the machine shown in figure 12 (b) was designed to test strips of the material in bending. The strips are first coiled somewhat like a watch spring and tested in this form; this feature

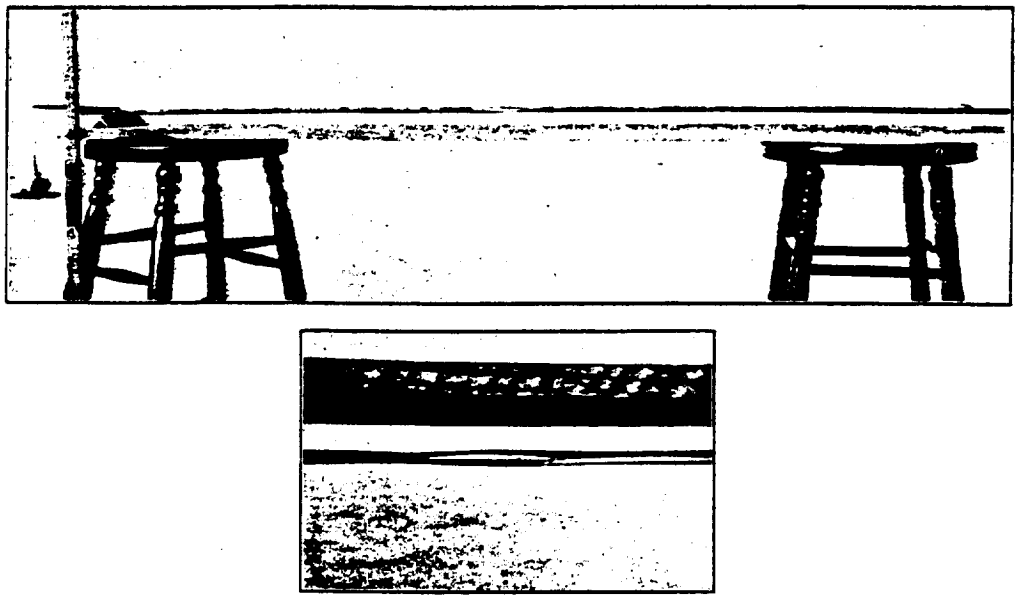

FIGURE 10.—Method of testing very long tubes and close-up of failure.

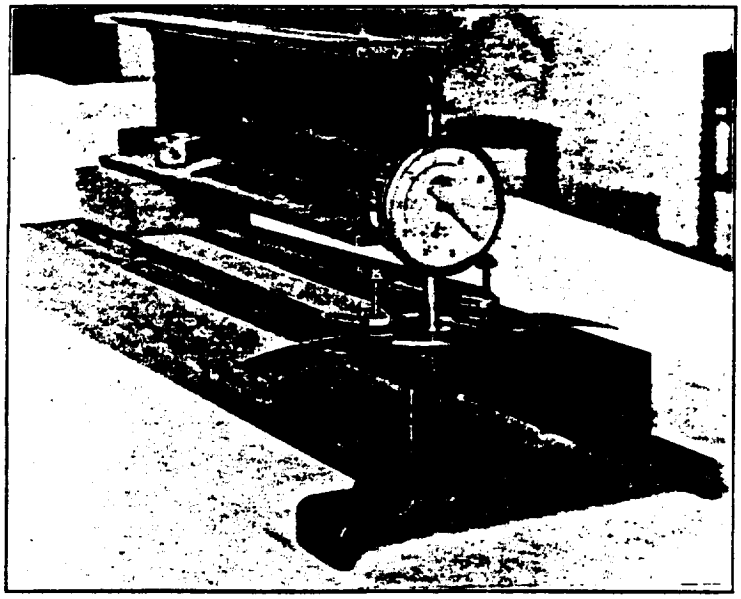

FIGURE 11.—Thickness tester.

for preventing all motions but the desired one; it is balanced to prevent bending the specimen, and its weight is allowed for by the proper initial setting of the load dial. It reads directly in 1/100,000 unit strain and can be read consistently to one tenth of this value

is necessary to insure straight cross sections. The machine exerts a pure couple on the coil, bending it uniformly through its length, and measures the total angle of bending. Very consistent results can be obtained. As the width of the strip is several hundred

times the thickness, this machine of course measures $E/(1-\mu^2)$, while the tension machine measures E. Assuming $\mu=0.3$ the values of E obtained from the two machines are found to check within 1 or 2 percent, and are very consistent for each type of material.

Data for all the tests are given in table I. In all cases the torque given is the maximum torque that the tube will take. In most cases, this ultimate torque was very sharply defined and occurred when the buckling deflection was comparatively small. In the case of the few extremely short tubes, however, the torque increased gradually for a long time after buckling started, the maximum value being reached when the buckling deflections were very deep. This seems to indicate that for such extremely short tubes, while the present theory presumably gives a correct value for the torque at which buckling would *start* if there were no eccentricities, the *ultimate* torque which the tube will take is probably to some extent a function of the elastic limit or yield point of the material. In the specimens tested, the strengthening effect of large deflections evidently counterbalanced to a great extent the weakening effect of initial eccentricities.

In many tests, buckling occurred only part way around the tube, and in these cases n was taken as the circumference divided by the average width of the circumferential waves. The value of θ was estimated roughly by eye, with the aid of a transparent protractor, from the appearance of the top or outermost part of the wave. The angle of the top and bottom of the wave must be the same when buckling starts but, as buckling increases, the angle at the bottom of the wave becomes greatly distorted, while the angle at the top seems to remain nearly constant.

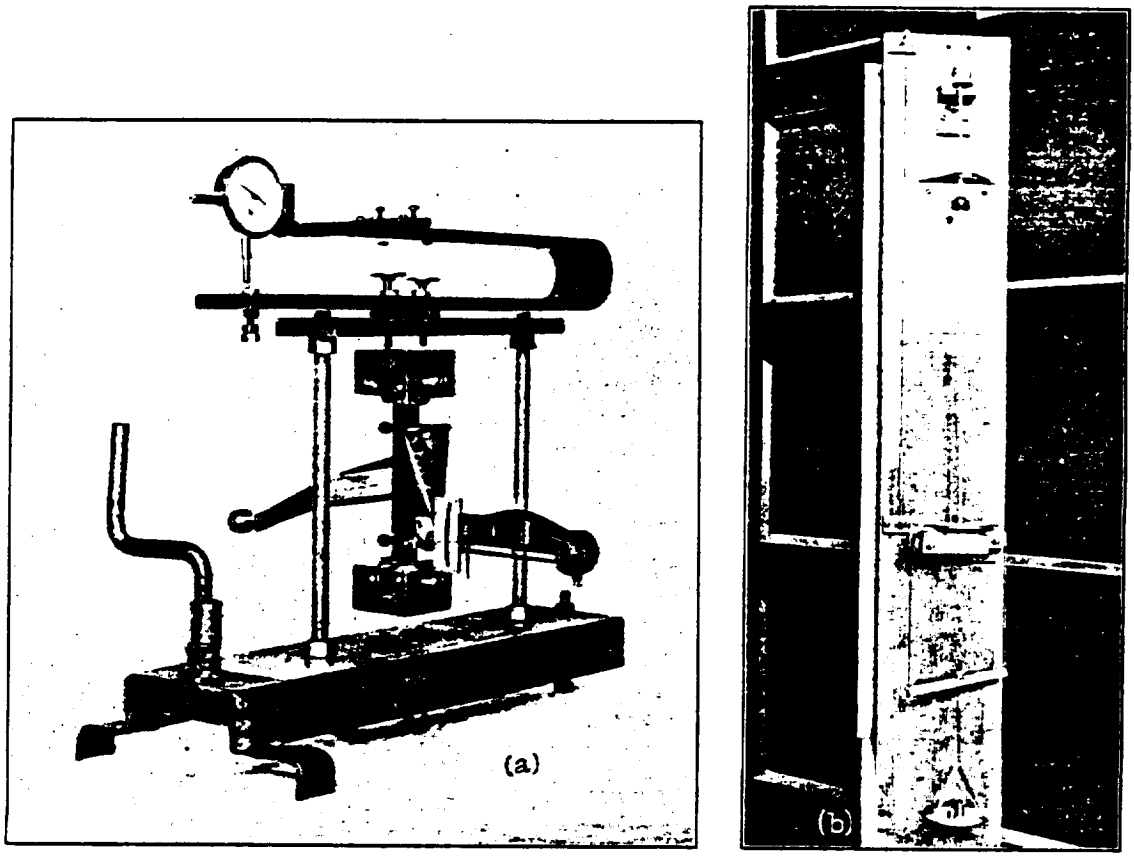

FIGURE 12.—Tensile and bending material testing apparatus.

In plotting the experimental results, μ is assumed to be 0.3 for metal tubes, 0.36 for celluloid, and 0.5 for rubber models.

DERIVATION OF THE EQUATIONS OF EQUILIBRIUM OF A CYLINDER WALL

The equations of equilibrium of elements of the cylindrical wall of the tube have been obtained in a new and simplified form; consequently it will be necessary to give a derivation. Figure 13 shows the coordinates and the components of displacement of the middle surface of the wall during buckling. A circumferential coordinate s is used in preference to an angular one, because it results in simpler expressions and makes the connection between a curved plate and the limiting case of a flat plate more readily seen. It will be shown

that, to the order of approximation which we need, it makes no difference whether the component of displacement v is considered to be measured circumferentially or tangentially.

The equations of equilibrium for a flat plate are well known, but the corresponding equations for the case of a curved plate are by no means so clearly established. In the case of a flat plate, in some problems only extensional strains or stresses—tension, compression, or shear in the plane of the plate—need be considered, while in other problems only flexure—bending or twisting—is of any importance. Extension and flexure may be considered separately, even in the case of a complex problem involving both; an exception to this is the case where large deflections occur to a non-developable surface. In the case of a curved plate, extension and flexure are, in general, interconnected even when the lateral deflections are of infinitesimal order. If no simplifications were made the conditions of equilibrium would be too complex to be

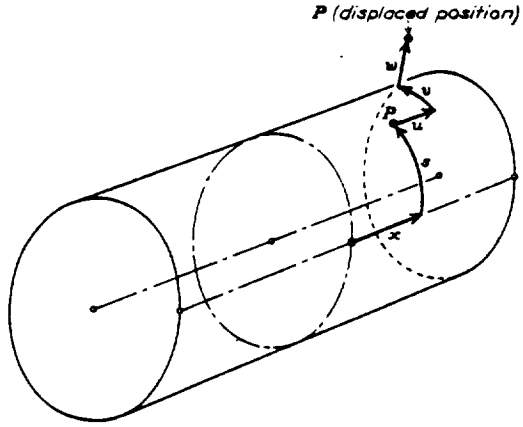

FIGURE 13.—Coordinates and components of displacement.

of much practical use. Much confusion seems to exist as to what simplifications can be made, and the conditions under which they can be made. One author considers items which another rejects as negligible, and vice versa. An attempt is made, in the following discussion, to clarify this question and to obtain the greatest simplification possible, under the conditions of the present problem; the results are applicable to a large class of problems.

The usual assumptions are made, that the material is perfectly elastic, that the tube is exactly cylindrical, that the wall thickness is small compared to the radius, and that the deflections are small compared to the thickness. The usual assumption is also made that straight lines in the cylinder wall, perpendicular to the middle surface, remain straight and perpendicular to the middle surface; that is, we neglect the distortion due to transverse shear. We could easily justify this assumption by taking the magnitude of the transverse shear, obtained on this assumption, as a first approximation and calculating a correction. The correction will be found to be negligible.

If lines perpendicular to the middle surface remain so during distortion then the displacement of *all* points in the cylinder wall can be found from the displacements of the middle surface u, v, and w. The equations of equilibrium can then be derived in terms of u, v, and w by considering: first, the purely geometrical relationship between these displacements and the strains in all parts of the wall; next, the relationship between the strains and the stresses, given by Hooke's and Poisson's relations; and last, the relationship between all the stresses on an element of the wall, given by the laws of equilibrium. There is no essential difficulty in doing this. However, as the contention to be made is that most writers consider more items than necessary, it will be sufficient to take their results and show what can be neglected.

Let us consider first the items that all authorities agree cannot be neglected. The extensional and flexural strains in the middle surface are

$$\epsilon_x = \frac{\partial u}{\partial x},\quad \epsilon_s = \frac{\partial v}{\partial s} + \frac{w}{r},\quad \epsilon_{xs} = \frac{\partial u}{\partial s} + \frac{\partial v}{\partial x}$$
$$\kappa_x = \frac{\partial^2 w}{\partial x^2},\quad \kappa_s = \frac{\partial^2 w}{\partial s^2},\quad \kappa_{xs} = \frac{\partial^2 w}{\partial x\,\partial s} \qquad (5)$$

These expressions are the same as the well-known expressions for the case of a flat plate, with the addition of w/r to the expression for ϵ_s. This term is due to the change in circumferential dimensions with change in the radius, which produces the strain:

$$\frac{r+w}{r} - 1 = \frac{w}{r}$$

The resultant forces and moments per unit length of wall section, obtained by summing up the stresses over the thickness, are taken as shown in figure 14. The relation between these and the strains of the middle surface will be taken the same as in the case of a flat plate:

$$T_x = \frac{Et}{1-\mu^2}(\epsilon_x + \mu\epsilon_s),\quad T_s = \frac{Et}{1-\mu^2}(\epsilon_s + \mu\epsilon_x),$$
$$T_{xs} = T_{xs}' = \frac{Et}{2(1+\mu)}\epsilon_{xs},\quad G_x = \frac{Et^3}{12(1-\mu^2)}(\kappa_x + \mu\kappa_s), \qquad (6)$$
$$G_s = \frac{Et^3}{12(1-\mu^2)}(\kappa_s + \mu\kappa_x),\quad G_{xs} = G_{xs}' = \frac{Et^3}{12(1+\mu)}\kappa_{xs}$$

We will now set up the conditions for equilibrium of an element such as shown in figure 14. Before doing this we must remember that we have taken u, v, and w as the displacements occurring *during buckling*, and hence the above quantities T_x, G_x, etc., represent only the *changes* in the internal forces during buckling. The total internal forces at any instant are the internal forces present before buckling, plus these changes.

In the particular problem that we are considering, the tube is subjected to torsion and, if the tube is perfectly cylindrical and uniform, the stress distribution and the distortion will be, before buckling begins, the same as assumed in elementary mechanics. There will be a shearing stress S on normal and longitudinal sections, which can be taken as uniform throughout the entire tube, since t/r is small. There will be a simple distortion in the circumferential direction, which leaves the tube still cylindrical and is of no interest to us. To obtain the total internal forces we must add to those shown in figure 14, the forces per unit length St, which will be considered to be in the opposite sense to T_{xs} and T_{xs}'.

In setting up the conditions of equilibrium of the element we must take into consideration the changes in the angles of its faces due to its distortion, as this will obviously affect the components of the forces in the different equilibrium equations. However, if the displacements are small this effect will be small, and its effect on T_x, G_x, etc., is of a second order of smallness compared to other items. But its effect on St

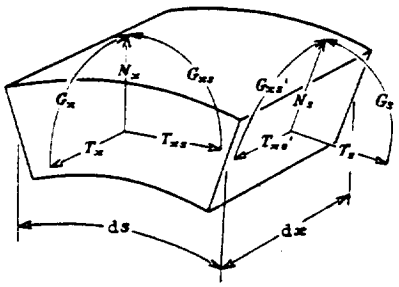

FIGURE 14.—Forces and moments on element of wall.

may be of the same order of magnitude as these other items, because St is an order of magnitude larger than T_x, G_x, etc.; the latter forces are proportional to the buckling displacements and when these displacements are small, T_x, G_x, etc., must be small compared to St, which had a finite value when the buckling started.

The terms which we will consider in the equations of equilibrium give, after simplification

$$\Sigma F_x = \frac{\partial T_x}{\partial x} + \frac{\partial T_{xs}'}{\partial s} = 0$$

$$\Sigma F_s = \frac{\partial T_s}{\partial s} + \frac{\partial T_{xs}}{\partial x} = 0$$

$$\Sigma F_r = \frac{\partial N_x}{\partial x} + \frac{\partial N_s}{\partial s} + \frac{T_s}{r} + 2St\frac{\partial^2 w}{\partial x \partial s} = 0 \qquad (7)$$

$$\Sigma M_x = \frac{\partial G_s}{\partial s} + \frac{\partial G_{xs}}{\partial x} - N_s = 0$$

$$\Sigma M_s = \frac{\partial G_x}{\partial x} + \frac{\partial G_{xs}'}{\partial s} - N_x = 0$$

There is no use in writing the equation of moments about the radial direction, as it would merely state what we have already assumed—that $T_{xs} = T_{xs}'$.

The term T_s/r in the third equation comes from the resultant of the force $T_s dx$ and the similar force on the opposite face of the element, due to the angle ds/r between them; this is the only term we will consider due to this angle, that is, due to the *curvature* of the element; all the other terms in (7) are the same as for a flat plate. The term $2St\frac{\partial^2 w}{\partial x \partial s}$ is the only term considered due to the distortion of the element; this is the resultant of forces $Stdx$ or $Stds$ on all four sides of the element, due to the angle of twist between opposite sides, $\frac{\partial^2 w}{\partial x \partial s}\,dx$ or $\frac{\partial^2 w}{\partial x \partial s}\,ds$. The rest of the terms in (7) are due to changes in T_x, G_x, etc., over the distances dx or ds, and to obvious moments due to N_x and N_s, the same as for a flat plate.

Using the last two equations to eliminate N_x and N_s from the third, replacing T_x, G_x, etc., by their values in (6), and then ϵ_x, κ_x, etc., by their values in (5), we obtain three equations involving: derivatives of u, v, and w with respect to x and s, the unknown S, and the physical constants of the tube

$$\frac{\partial^2 u}{\partial x^2} + \frac{1-\mu}{2}\frac{\partial^2 u}{\partial s^2} + \frac{1+\mu}{2}\frac{\partial^2 v}{\partial x \partial s} + \frac{\mu}{r}\frac{\partial w}{\partial x} = 0$$

$$\frac{\partial^2 v}{\partial s^2} + \frac{1-\mu}{2}\frac{\partial^2 v}{\partial x^2} + \frac{1+\mu}{2}\frac{\partial^2 u}{\partial x \partial s} + \frac{1}{r}\frac{\partial w}{\partial s} = 0 \qquad (8)$$

$$\frac{t^2}{12}\nabla^4 w + \frac{1}{r}\left(\frac{\partial v}{\partial s} + \mu\frac{\partial u}{\partial x} + \frac{w}{r}\right) + \frac{2(1-\mu^2)S}{E}\frac{\partial^2 w}{\partial x \partial s} = 0$$

where $\nabla^2 = \frac{\partial^2}{\partial x^2} + \frac{\partial^2}{\partial s^2}$, and ∇^4 signifies that this operator is to be applied twice.

Equations (8) can be simplified as follows: Applying first $\frac{\partial^2}{\partial x^2}$ and then $\frac{\partial^2}{\partial s^2}$ to the first equation, solving in each case for the term involving v, and substituting these expressions in the equation obtained by applying $\frac{\partial^2}{\partial x \partial s}$ to the second equation, we obtain an equation from which v has been eliminated. Similarly, applying $\frac{\partial^2}{\partial x^2}$ and $\frac{\partial^2}{\partial s^2}$ to the second equation, solving for the term involving u, and substituting in the first equation, after applying $\frac{\partial^2}{\partial x \partial s}$ to it, we obtain an equation from which u has been eliminated. These equations are, after simplification:

$$r\nabla^4 u = -\mu\frac{\partial^3 w}{\partial x^3} + \frac{\partial^3 w}{\partial x \partial s^2}$$

$$r\nabla^4 v = -(2+\mu)\frac{\partial^3 w}{\partial x^2 \partial s} - \frac{\partial^3 w}{\partial s^3} \qquad (9)$$

Now, applying $\frac{\partial}{\partial x}$ to the first of these equations and $\frac{\partial}{\partial s}$ to the second, and substituting in the equation obtained by applying ∇^4 to the third equation of (8),

we obtain an equation from which both u and v have been eliminated:

$$\frac{Et^3}{12(1-\mu^2)}\nabla^8 w+\frac{Et}{r^2}\frac{\partial^4 w}{\partial x^4}+2St\nabla^4\left(\frac{\partial^2 w}{\partial x\partial s}\right)=0 \quad (10)$$

Equation (10) is the same as the corresponding equation for a flat plate, with the exception of the second term; this is evident if we set r infinite in (10). The contention being made is that this term represents the principal effect of the curvature in a large class of problems of which the present problem is one. For most problems, equation (10) represents the complete equilibrium condition. However, if it is desired to include constraints against u and v displacements in the boundary conditions (as will be done here), relations (9) must be used for this purpose; this, of course, constitutes another effect of the curvature, but it will be a very small effect in most cases.

In using these simplified results for other problems, it is only necessary to remember that the last term of equation (10) represents the radial force on the cylinder wall due to the loading, per unit area of the wall, to which the operator ∇^4 is applied. Thus for the problem of the buckling of a cylinder wall under axial compressive stresses, S_x (due to an axial load or due to bending), equations (9) and (10) will be as above except that the last term of (10) will be $t\nabla^4\left(S_x\frac{\partial^2 w}{\partial x^2}\right)$. For a tube under a varying external pressure p, this last term will be $\nabla^4 p$ (but if p is constant with respect to s, or varies very gradually, then the above equations may be no longer applicable, as will be explained later). For studying lateral vibrations of the cylinder wall, the last term of (10) will be $m\nabla^4\ddot{w}$, where m is the mass per unit area and $\ddot{w}$ is the second derivative of w with respect to time.

It is necessary now to justify the neglect, in deriving (9) and (10), of many items which are commonly considered. In the relations between strains and displacements (5), we neglected, in the expression for κ_x, a term $\frac{1}{r^2}w$, due to change of curvature with change of radius. If v is measured tangentially the expression for κ_s should logically include also the term $\frac{1}{r}\frac{\partial v}{\partial s}$; if v is measured circumferentially this is unnecessary, but κ_{xs} should have an additional term $\frac{1}{r}\frac{\partial v}{\partial x}$. As for expressions (6) for the internal forces and moments in terms of the strains of the middle surface, we have obviously neglected the effect of the variation in the length of circumferential fibers along the thickness. Love (reference 9) gives a second approximation for the internal forces, in which the expressions for G_x, G_s, G_{xs}, and G_{xs}' are the same as in (6), but the expressions for T_x, T_s, T_{xs}, and T_{xs}' contain a number of additional terms involving the flexural strains κ_x, κ_s, and κ_{xs}. In these expressions T_{xs} and T_{xs}' are no longer equal, but have values satisfying a more exact statement of the equation of equilibrium of moments on an element, about the radial direction.

In setting up the equilibrium conditions (7), many terms were neglected. It has been noted that the term T_s/r in the third equation comes from the resultant of the T_s forces on opposite faces of the element, due to the angle ds/r between these faces. By the same reasoning, there should logically be a term N_s/r in the second equation, and a term G_{xs}'/r in the equation of equilibrium of moments about the radial direction, as noted in the last paragraph. The term $2St\frac{\partial^2 w}{\partial x\partial s}$ in the third equation represents the radial components of St forces on opposite faces of the element, due to the angle $\frac{\partial^2 w}{\partial x\partial s}dx$ or $\frac{\partial^2 w}{\partial x\partial s}ds$ between them. There are other small angles between the St forces on the opposite faces, produced by distortion of the element, and these give resultants in the x and s directions; these are considered by Schwerin (reference 5) in his solution of the torsion problem.

The justification for neglecting all these items lies in the following: If any, or all, of them are included, we obtain finally an equation corresponding to (10), which includes all the terms in (10) and numerous additional terms. Now suppose we take w as a harmonic function of s, such as the expression (13), given later, for which n represents the number of circumferential waves of the displacement, and substitute it in this equation. If we compare the two types of terms which we obtain—those which we would get with (10) and the additional terms—we find that each of the additional terms is equal to a term we get with (10) multiplied by $(t/r)^2$ or $1/n^2$, and with some numerical factor of the order of unity. Those involving $(t/r)^2$ can be immediately thrown out, for any "thin-walled" cylinder. Those involving $1/n^2$ can evidently be neglected when n is large. This means that (10) is applicable in all thin-wall problems in which the deformation consists of a large number of waves in the circumferential direction, or in which it changes rapidly in this direction.

It is an interesting fact that a simple test exists for differentiating between items which can be neglected on the above basis and those which cannot be, in the expressions for ϵ_x, κ_x, etc., for T_x, G_x, etc., or in the equilibrium equations. If we make the substitution $u=\sqrt{t/r}\,u'$, $v=\sqrt{t/r}\,v'$, $x=\sqrt{tr}\,x'$, $s=\sqrt{tr}\,s'$ and divide all the items by the proper factor, we find that items which can be neglected are left with a factor t/r, while the other items are free from such a factor. For

example, suppose we wish to compare the items in the expression

$$\kappa_s = \frac{\partial^2 w}{\partial s^2} + \frac{1}{r^2} w + \frac{1}{r} \frac{\partial v}{\partial s}$$

Making the above substitution, we find

$$\kappa_s = \frac{1}{tr} \left(\frac{\partial^2 w}{\partial s'^2} + \frac{t}{r} w + \frac{t}{r} \frac{\partial v'}{\partial s'} \right)$$

The meaning of this is probably that, for the class of problems to which (10) applies, u and v are of the order of magnitude of $\sqrt{\frac{t}{r}}\, w$.

One more question requiring discussion is that of how large n must be in order for (10) to give a reasonably accurate result. In the present problem the results obtained from (10) give an excellent check with experiments when n is only 2. (See fig. 2.) Moreover, the results seem to check reasonably with those of Schwerin, who used a number of the items neglected in (10), indicating that these items were of minor importance even when $n=2$. On the other hand, the results obtained from (10) give an entirely distorted result when $n=1$. There seems to be a rather critical change between $n=1$ and $n=2$, for our particular problem at least.

It is no inconvenience to us that (10) is inapplicable when $n=1$, because for this case the cross section of the tube is entirely undistorted, merely undergoing a general displacement. The elementary theory of bending of a tube evidently applies in such a case, and there would hardly be any advantage in having a complex solution for a case to which elementary theory applies. However, borderline problems doubtless exist for which neither (10) nor an elementary treatment would be accurate. It cannot be concluded, however, that the equations of equilibrium commonly used, which take into consideration *some* of the items neglected in (10) but not all of them, will necessarily be more accurate in such a case than (10). Unless the equations of equilibrium take *all* such items into consideration they may quite possibly be less accurate than (10), rather than more accurate.

THE BOUNDARY CONDITIONS

There are only two boundary lines to a tube (the two ends), instead of the four which we have in rectangular plate problems. The boundary conditions which we would have for the lateral sides of a plate or for the edges of the split in the case of a split tube are replaced in the case of a complete tube by the condition that the displacements must be cyclical functions of s, with the cycle length πd.

We will consider two edge conditions at the ends. For the case of clamped edges we will assume all components of displacement, and the slope of the surface in the axial direction, to be zero. There must, of course, be a uniform circumferential displacement for at least one end while the torsion is being applied and before buckling takes place. However, we are considering only what takes place *during buckling*. We will find that our equations can be satisfied with S a constant, which means that S, and therefore the torque on the tube, remains constant during the buckling. There is therefore no reason for any relative circumferential displacement of the ends while buckling takes place, and the conditions for fixed edges are

$$x = \pm \frac{l}{2}: \quad u = v = w = \frac{\partial w}{\partial x} = 0 \tag{11}$$

Similarly, the condition for hinged edges at the ends is that the components of displacement and the moment G_x are zero:

$$x = \pm \frac{l}{2}: \quad u = v = w = \frac{\partial^2 w}{\partial x^2} + \mu \frac{\partial^2 w}{\partial s^2} = 0 \tag{12}$$

Both of the above end conditions evidently require, not only that the edges of the tube shall be clamped or hinged, say to some rigid end piece, but that the ends *as a whole* shall have no linear or angular motion relative to each other. However, if we take the final results obtained, and calculate the resultant of all the forces on the end of the tube due to buckling, (that is, the resultant of T_x, T_{xs}, N_x, G_x, and G_{xs}, when $x = \frac{l}{2}$ or $x = -\frac{l}{2}$) we find this resultant to be zero. This means that no constraints are required to prevent motion of the ends of the tube as a whole; that is, it makes no difference whether or not they are free to move as a whole (this does not apply to the case $n=1$, which is discussed later).

THE SOLUTION

The equations of equilibrium and the boundary conditions are satisfied if $u=v=w=0$—an obvious solution of no interest to us. Buckling displacements are *other* types of displacement which satisfy these conditions. There are many such displacements and each one requires a certain definite value of S. Our problem is to find the lowest of such values of S for each given tube; buckling will certainly take place as soon as S exceeds this value. In the present problem the equilibrium and boundary conditions can be satisfied if S is a constant with respect to the displacements, and the displacements are the following functions of x and s:

$$\begin{aligned} u &= \sum_m U_m \sin 2\left(n\frac{s}{d} + \lambda_m \frac{x}{l}\right) \\ v &= \sum_m V_m \sin 2\left(n\frac{s}{d} + \lambda_m \frac{x}{l}\right) \\ w &= \sum_m W_m \cos 2\left(n\frac{s}{d} + \lambda_m \frac{x}{l}\right) \end{aligned} \tag{13}$$

where U_m, V_m, W_m, and n are real numbers, n being an integer, and λ_m may be complex. Substituting these values in (9) and (10), we obtain

$$U_m = \frac{W_m}{n}\frac{\lambda_m}{k}\frac{1-\mu\left(\frac{\lambda_m}{k}\right)^2}{\left[1+\left(\frac{\lambda_m}{k}\right)^2\right]^2}$$
$$V_m = -\frac{W_m}{n}\frac{1+(2+\mu)\left(\frac{\lambda_m}{k}\right)^2}{\left[1+\left(\frac{\lambda_m}{k}\right)^2\right]^2} \quad (14)$$

$$k^8\left[1+\left(\frac{\lambda_m}{k}\right)^2\right]^2+3\left[\frac{H}{1+\left(\frac{\lambda_m}{k}\right)^2}\right]^2\lambda_m^4-6A^2k^6\lambda_m=0 \quad (15)$$

The summation signs have been dropped. If these equations are satisfied without the summation signs, they will certainly be satisfied with them.

If we now substitute (13) and (14) in the eight boundary conditions (11) or (12), and eliminate s from these equations in a similar manner to that used later, we obtain eight linear equations in W_1, W_2, W_3, etc. As there are no terms not containing W_m, it will take eight values of W_m, which means eight terms in the summations of (13), as well as a determinantal relation, to satisfy them. This determinantal equation involves the eight values of λ_m. As (15) is of eighth degree in λ_m, for a given set of values of k, H, and A, λ_m may have in general eight different values. It can easily be shown that under these conditions the determinantal equation and (15) together determine a relation between k, H, and A. The problem is to determine this relationship; it is not impossible to do it, but the algebraic complexities of the problem render it impracticable.

We will therefore make certain minor approximations that will make the problem more tractable. The results of experiments give the clue for doing this. It is evident from (13) that $\frac{\lambda_m d}{n\,l}=\frac{\lambda_m}{k}$ is the tangent of the angle of deflection waves with the axial direction. From the theory of Southwell and Skan (reference 6) and from experiments, we know that the angle θ starts at about 45° for infinitely short cylinders and rapidly decreases as the length increases, being about 15° when the length equals the diameter, and evidently approaching zero at very large length/diameter ratios (of course, we will show that θ is a function of H, rather than of l/d, but the foregoing statement is justified by the fact that d/t has a practical lower limit determined by the elastic limit of available materials).

This indicates that, for all except very short tubes, λ_m/k is small compared to 1. Of course, the actual deformation is a superposition of eight deformations, each with a different value of λ_m/k; some of the values of λ_m/k may not be small, but experiments as well as the following theory show that the *important* values of λ_m/k are certainly small, except when l/d is small. We are also quite safe in assuming that λ_m/k approaches zero for large values of l/d, as this assumption certainly gives a good first approximation, and this first approximation vertifies the assumption.

These facts are the basis for the approximations which we will use. Starting with (14), if we neglect $\left(\frac{\lambda_m}{k}\right)^2$ in comparison to 1, we obtain

$$U_m = \frac{W_m}{n}\frac{\lambda_m}{k}$$
$$V_m = -\frac{W_m}{n} \quad (16)$$

The error introduced by this approximation is zero at both extremes, when l/d is infinite, and also when $l/d=0$—because both U_m and V_m are then zero anyway, since n becomes infinite. The error is small for any intermediate case because when λ_m/k is not small compared to 1, n is large and U_m and V_m are of little importance. For example, when $l/d=1$, taking $\lambda_m/k=\tan 15°$, the error in V_m is about 3 percent, and in U_m (which is much less important than V_m, as it contains the factor λ_m/k) about 14 percent. Moreover, investigation of the final results shows that U_m is never of any particular importance, and even V_m is not important here, only becoming of importance when l is large compared to d.

Substituting (13) and (16) in (11) or (12), and dividing through by common factors, we find, for $x=\pm\frac{l}{2}$:

$$\left.\begin{aligned} v=0:&\ \Sigma W_m \sin\left(n\tfrac{s}{r}\pm\lambda_m\right)=0 \\ w=0:&\ \Sigma W_m \cos\left(n\tfrac{s}{r}\pm\lambda_m\right)=0 \quad \text{(both edge conditions)} \\ u=0:&\ \Sigma W_m\lambda_m \sin\left(n\tfrac{s}{r}\pm\lambda_m\right)=0 \\ \frac{\partial w}{\partial x}=0:&\ \Sigma W_m\lambda_m \sin\left(n\tfrac{s}{r}\pm\lambda_m\right)=0 \quad \text{(clamped edges)} \\ G_z=0:&\ \Sigma W_m\lambda_m^2 \cos\left(n\tfrac{s}{r}\pm\lambda_m\right)=0 \quad \text{(hinged edges)} \end{aligned}\right\} \quad (17)$$

We will neglect the third condition for hinged edges, that $u=0$. This is by far the least important of the four conditions, owing to the relative insignificance of U_m, as mentioned before. Neglecting this condition, and using the trigonometric formulas for the sines and cosines of the sum of two numbers, we obtain

$$\left.\begin{aligned} &\sin n\frac{s}{r}(\Sigma W_m \cos \lambda_m) \\ &\pm\cos n\frac{s}{r}(\Sigma W_m \sin \lambda_m)=0 \\ &\sin n\frac{s}{r}(\Sigma W_m \sin \lambda_m) \\ &\pm\cos n\frac{s}{r}(\Sigma W_m \cos \lambda_m)=0 \end{aligned}\right\}\text{(both edge conditions)}$$

$$\left.\begin{aligned} &\sin n\frac{s}{r}(\Sigma W_m\lambda_m \cos \lambda_m) \\ &\pm\cos n\frac{s}{r}(\Sigma W_m\lambda_m \sin \lambda_m)=0 \end{aligned}\right\}\text{(clamped edges)}$$

$$\left.\begin{aligned} &\sin n\frac{s}{r}(\Sigma W_m\lambda_m^2 \sin \lambda_m) \\ &\pm\cos n\frac{s}{r}(\Sigma W_m\lambda_m^2 \cos \lambda_m)=0 \end{aligned}\right\}\text{(hinged edges)}$$

All these conditions will be satisfied if

$$\left.\begin{aligned} &\left.\begin{aligned} &\Sigma W_m \sin \lambda_m=0 \\ &\Sigma W_m \cos \lambda_m=0 \\ &\Sigma W_m\lambda_m \cos \lambda_m=0 \\ &\Sigma W_m\lambda_m \sin \lambda_m=0 \end{aligned}\right\}\text{(clamped edges)} \\ &\left.\begin{aligned} &\Sigma W_m \sin \lambda_m=0 \\ &\Sigma W_m \cos \lambda_m=0 \\ &\Sigma W_m\lambda_m^2 \cos \lambda_m=0 \\ &\Sigma W_m\lambda_m^2 \sin \lambda_m=0 \end{aligned}\right\}\text{(hinged edges)} \end{aligned}\right\} \qquad (18)$$

These four equations for each end condition can be satisfied by four values of W_m, that is four terms to the summations of (13), and a determinantal relationship involving the λ_ms. The conditions (18) are the same as the boundary conditions found by Southwell and Skan (reference 6) for the case $l/d=0$. These writers show that the determinantal relationships between the λ_ms, implied by (18), can be put in the following forms:

$$\left.\begin{aligned} &\left.\begin{aligned} &(\lambda_1-\lambda_2)(\lambda_3-\lambda_4)\sin(\lambda_1-\lambda_3) \\ &\sin(\lambda_2-\lambda_4)=(\lambda_1-\lambda_3)(\lambda_2-\lambda_4) \\ &\sin(\lambda_1-\lambda_2)\sin(\lambda_3-\lambda_4) \end{aligned}\right\}\text{(clamped edges)} \\ &\left.\begin{aligned} &(\lambda_1^2-\lambda_2^2)(\lambda_3^2-\lambda_4^2)\sin(\lambda_1 \\ &-\lambda_3)\sin(\lambda_2-\lambda_4)=(\lambda_1^2 \\ &-\lambda_3^2)(\lambda_2^2-\lambda_4^2)\sin(\lambda_1 \\ &-\lambda_2)\sin(\lambda_3-\lambda_4) \end{aligned}\right\}\text{(hinged edges)} \end{aligned}\right\} \qquad (19)$$

We will next use the fact that λ_m/k is small compared to 1 (except for small values of l/d) to reduce the equilibrium equation (15) to one of the fourth degree in λ_m. This can be done in several ways. The most accurate is to merely consider $H\Big/\left[1+\left(\frac{\lambda_m}{k}\right)^2\right]=H'$ as a quantity independent of λ_m, until we obtain a solution. This gives

$$(k^4+3H'^2)\lambda_m^4+2k^6\lambda_m^2-6Ak^5\lambda_m+k^8=0 \qquad (20)$$

The error introduced is zero for the extreme cases, when $l/d=\infty$ (since $\lambda_m/k=0$), and when $l/d=0$, since $H=0$ for this case. For intermediate cases, a fair first approximation for the value of A, and therefore of S, could be expected even if we neglected λ_m/k altogether in the above quantity, taking $H'=H$, because when the error in neglecting λ_m/k is large, H is small and the whole second term in (15) is of small importance in determining A; when this term is important λ_m/k is small compared to one, and the error is small.

A second approximation for the relation between S and H is obtained by taking

$$H=H'\left(1+\frac{\lambda_m^2}{k^2}\right) \qquad (21)$$

where λ_m^2 is taken as a weighted average of the four values found in the first approximation. In figure 1 the relation between A and H, for clamped edges, obtained from the first approximation, is shown by the dotted line, while the second approximation is shown in full line. The difference between the values of A or S found from the first and from the second approximation is never more than about 20 percent (and is much less than this in the range of greatest practical importance). Hence, if general experience is a safe guide, the maximum error in the second approximation is probably not more than a few percent. This is borne out by the tests, as the average ratio of experimental to theoretical results is about the same in the range where the theory is most uncertain, as it is in the more certain range.

A further simplification of (15) can be obtained by completely neglecting $(\lambda_m/k)^2$ in comparison to one in both the first and second terms. Equation (15) then reduces to

$$3\lambda_m^4-6n^5BJ\lambda_m+n^5J^2=0 \qquad (22)$$

This would give a very poor approximation for very short tubes, but it is an excellent approximation for long tubes for which λ_m/k is small, and the error becomes zero when $l/d=\infty$. Due to the absence of a term in λ_m^2 this equation is much easier to work with than (20), and we can obtain most of our results from it, using (20) only to fill in the theory for very short tubes. The results obtained from (22) are shown in figure 2, and also give the straight upper portions of the curves in figure 1. Equation (20) yields the lower portions of these curves, which approach asymptotically the straight lines given by (22).

As (20) and (22) are of fourth degree in λ_m, they are in general satisfied by four values of λ_m, that is, four roots of the equation, for any given set of values of k, H, and A or n, J, and B. But these four values of λ_m must also satisfy the boundary condition (19), and in general this can only be done if certain relations exist between k, H, and A or n, J, and B. The problem is to find these relations; when we have them we still have the task of selecting the values of n or k which give the lowest S for any given tube, as buckling can occur when this S is reached.

As the term in λ_m^3 is absent in both (20) and (22) we know that $\lambda_1+\lambda_2+\lambda_3+\lambda_4=0$. From the results of Southwell and Skan (reference 6) we know that for the case $l/d=0$, two of these roots are real, and the other two complex with the real part negative. Trial shows this to be true for all values of l/d. We can therefore express the roots as follows:

$$\lambda_1=a+b,\ \lambda_2=a-b,\ \lambda_3=-a+ic,\ \lambda_4=-a-ic \qquad (23)$$

where a, b, and c are positive real numbers. The equation of which these are the roots is

$$[\lambda_m-(a+b)][\lambda_m-(a-b)][\lambda_m-(-a+ic)][\lambda_m-(-a-ic)]=$$
$$\lambda_m^4-(2a^2+b^2-c^2)\lambda_m^2-2a(b^2+c^2)\lambda_m+(a^2-b^2)(a^2+c^2)=0$$

Equating the coefficients in this equation to those in (20) we find the following conditions which must be satisfied:

$$2a^2+b^2-c^2=-\frac{2k^6}{k^4+3H'^2}$$
$$a(b^2+c^2)=\frac{3Ak^5}{k^4+3H'^2} \qquad (24)$$
$$(a^2-b^2)(a^2+c^2)=\frac{k^8}{k^4+3H'^2}$$

or if (22) is used

$$2a^2+b^2-c^2=0$$
$$a(b^2+c^2)=n^5BJ \qquad (25)$$
$$3(a^2-b^2)(a^2+c^2)=n^8J^2$$

These three equations from the equilibrium condition (24) or (25), must be solved with a fourth given by the boundary conditions. This is obtained by substituting (23) in (19); the results can be put in the following form:

$$4a^2=b^2-c^2+\frac{2bc}{N\tan 2b} \quad \text{(clamped edges)}$$
$$4a^2=\frac{(b^2+c^2)^2}{b^2-c^2-\frac{2bc}{N\tan 2b}} \quad \text{(hinged edges)} \qquad (26)$$

where $N=\dfrac{\tanh 2c}{1-\dfrac{\cos 4a}{\cos 2b\cosh 2c}}\approx 1$. Trial shows that $2c$ is never less than 6, and $2b$ varies between π and $\frac{7}{6}\pi$, for clamped edges, and between π and $\frac{5}{6}\pi$, for hinged edges, for the lowest range of real solutions for S (real solutions can also be obtained with values of $2b$ around 2π, 3π, etc., but these solutions give much higher values of S). For such a range of values, we can take $N=1$ without any appreciable error.

Consider now solutions obtained with (25) (which will apply to all but short tubes). Eliminating a between (26) and the first equation of (25), and assuming values for b between the limits mentioned above, we solve for the corresponding values of c. This can be done directly in the case of clamped edges, as we have a simple quadratic equation in c to work with; in the case of hinged edges, the values of c were found by a simple graphical method. The value of a can next be found from the first equation of (25), and then the values of n^8J^2 and n^5BJ from the last two equations. Table II shows various sets of values of all these quantities, thus obtained.

From the sets of values of n^8J^2 and n^5BJ we can calculate, for any given value of n (2, 3, 4, etc.) sets of corresponding values of J, and then B. In this way were plotted the families of curves, showing the relation between B and J for $n=2$, $n=3$, etc., in figure 2. Obviously, only the portion of each curve which is *below* the other curves, that is, the portion between intersections with the adjacent curves, has practical significance, as buckling will occur at the lowest stress at which equilibrium in a buckled state can exist. Hence, the relation between B and J (and therefore between S and the properties of the tube), when buckling occurs, is given by the jagged lines shown in the figure, made up of the lower portions of the curves for $n=2$, $n=3$, etc. As indicated on the figure, the intersections of the curves give the values of J at which the number of circumferential waves will change from one integer to the next. Thus a clamped edge tube for which $J>1.45$ should buckle in two waves; and for $1.45>J>0.35$ it should buckle in three waves, etc. It will be noted that test results are quite consistent with the theory in this respect.

The relation between n^5BJ and n^8J^2 can be very nearly expressed, for the range of values of actual significance, by the formulas: n^5BJ is equal to

$$\left.\begin{array}{ll} 0.385\ (n^8J^2)^{\frac{1}{2}}+.94\ (n^8J^2)^{\frac{1}{4}}+18.3 & \text{(clamped edges)} \\ 0.385\ (n^8J^2)^{\frac{1}{2}}+(n^8J^2)^{\frac{1}{4}}+6.5 & \text{(hinged edges)} \end{array}\right\} (27)$$

The values obtained from these expressions are shown in table II, in the column next to n^5BJ. These relations can be simplified to

$$\left.\begin{array}{ll} B=0.385\ nJ^{\frac{1}{2}}+\dfrac{0.94}{n^2J^{\frac{1}{4}}}+\dfrac{18.3}{n^5J} & \text{(clamped edges)} \\ B=0.385\ nJ^{\frac{1}{2}}+\dfrac{1}{n^2J^{\frac{1}{4}}}+\dfrac{6.5}{n^5J} & \text{(hinged edges)} \end{array}\right\} (28)$$

These are the equations of the individual curves in figure 2. For very large values of J, $n=2$ and only the first terms of (28) are important, giving us equation (2). This is the equation of the line eef in figure 2, which the curves for $n=2$ approach asymptotically. By equating the right-hand side of (28) to the same expression with n replaced by $n+1$, we obtain an equation for determining the value of J for which the number of circumferential waves changes from n to $n+1$.

It will be noticed that the part of the jagged lines in figure 2 corresponding to larger values of n approach closer and closer to the envelopes of all the curves, shown by the broken lines de. For values of J below

6 or 7 this envelope can be used instead of the jagged line without serious error. We can obtain the equation of this envelope very simply—merely by treating n as though it could have any value, fractional as well as integral. In the last column of table II, values of n^3J^2 have been raised to the ⅔ power and divided into corresponding values of n^3BJ, giving us values of

$$\frac{n^3BJ}{(n^3J^2)^{\frac{1}{2}}}=\frac{B}{J^{\frac{1}{2}}}$$

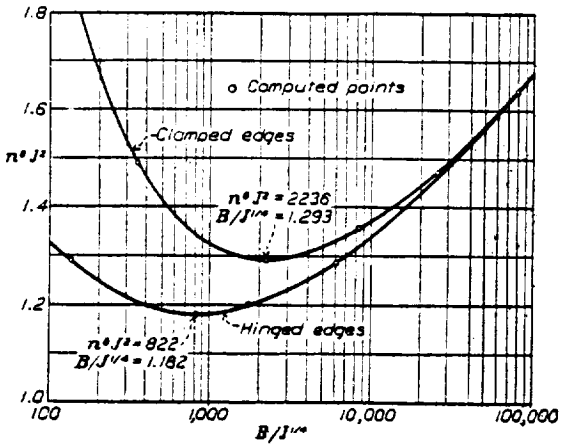

FIGURE 15.—Plot of n^6J^2 against $B/J^{1/6}$

These values have been plotted on figure 15. It will be seen that the minimum value of $B/J^{\frac{1}{2}}$—and therefore the minimum value of B for any given value of J—occurs when $n^3J^2=2236$ (clamped edges) or $n^3J^2=822$ (hinged edges), that is when

$$\left.\begin{aligned} n&=2236^{\frac{1}{6}}/J^{\frac{1}{2}}=2.62/J^{\frac{1}{2}}\ \text{(clamped edges)}\\ n&=822^{\frac{1}{6}}/J^{\frac{1}{2}}=2.31/J^{\frac{1}{2}}\ \text{(hinged edges)}\end{aligned}\right\} \quad (29)$$

These minimum values of $B/J^{\frac{1}{2}}$ are 1.29 for clamped edges, and 1.18 for hinged edges. Hence, the minimum B for any given J is

$$\left.\begin{aligned} B&=1.29\ J^{\frac{1}{2}}\ \text{(clamped edges)}\\ B&=1.18\ J^{\frac{1}{2}}\ \text{(hinged edges)}\end{aligned}\right\} \quad (30)$$

These are the equations of the envelopes in figure 2. Equations (29) give the approximate number of circumferential waves in which a tube will buckle; if n is taken as an integer, these equations give the intersections of the envelope with the corresponding curve. These equations can be put in a different form by multiplying (29) by l/d and (30) by $\sqrt{1-\mu^2}\frac{l}{t}$:

$$\begin{aligned} k&=2.62\ H^{\frac{1}{2}}\ \text{(clamped edges)}\\ k&=2.31\ H^{\frac{1}{2}}\ \text{(hinged edges)}\\ A&=1.29\ H^{\frac{1}{2}}\ \text{(clamped edges)}\\ A&=1.18\ H^{\frac{1}{2}}\ \text{(hinged edges)}\end{aligned}$$

In this form, they were used to plot the right hand end of the curves in figures 1 and 3.

We have assumed the minimum number of circumferential waves to be two. The case $n=0$ clearly has no significance for the torsion problem, but the case $n=1$ is not so obvious. This would give a distortion in which cross sections remain circular but are displaced, the displacement spiralling around the center line, so that the shape of the tube would become something like that of a corkscrew. Such a displacement can easily be obtained by twisting a long piece of rubber tubing in the hands; however, no such distortion has been observed in a thin-walled metal tube, even in the tube shown in figure 10, which had a length/diameter ratio of nearly 170.

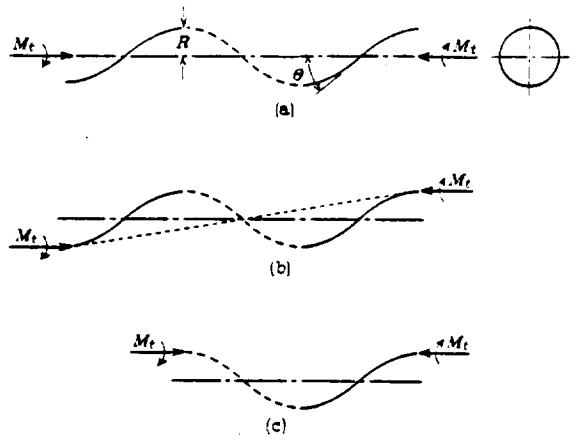

FIGURE 16.—The case $n=1$.

As previously explained, the equations of equilibrium that we have used do not apply to this case, but the elementary theory of bending of a tube does apply. Figure 16a shows a tube undergoing this type of distortion, under the action of a twisting moment M_t, the center line being bent to a spiral and having the constant angle θ with the axis of the spiral. If the couple M_t acts about the axis of the spiral, all parts of the tube will be subjected to the bending moment $M_t \sin\theta$. At the same time it can easily be shown that all parts of the tube are bent to a curvature $\sin^2\theta/R$ (where R is the radius of the spiral). This curvature is in the same plane as the bending moment $M_t \sin\theta$. Hence all parts of the tube will be in equilibrium if

$$M_t \sin\theta = EI\frac{\sin^2\theta}{R}$$

$$M_t = EI\frac{\sin\theta}{R} \quad (a)$$

If the end conditions are such that $\sin\theta/R$ can have only one particular value, as in the case discussed in the next paragraph, then this formula determines a value of M_t at which the tube can buckle in the shape given.

It was assumed above that the couple M_t is applied at the axis of the spiral. In a practical case it would

naturally be applied at the end of the tube, as shown in figure 16b. As the couple has only been moved parallel to itself this is statically equivalent to the case of figure 16a, and the above reasoning still applies. But now the couples at the ends of the tube are not about the line joining the two ends (shown dotted in the figure). In order to fullfil a requirement that the end couples be about this line, the spiral form of the tube must consist of an even number of full turns. The condition for this is that

$$\frac{\sin\theta}{R}=m\frac{2\pi}{l}$$

where m is an integer. Taking $m=1$, as in figure 16c, and substituting this in (a), we find

$$M_t=\frac{2\pi EI}{l}$$

This checks Greenhill's solution (reference 10) and the loading conditions correspond to those assumed by Greenhill. However, many other solutions could be obtained from (a) for other end conditions, and the special end conditions assumed by Greenhill are no closer to most practical cases than the others. In none of these cases could the loading applied be called a pure twisting moment, as the applied couple is not about the axis of the tube at the end, as it is for instance in the actual experiment shown in figure 10.

It would not be worth while, for most practical purposes, to try to obtain solutions for other end conditions such as that in figure 10, because a little figuring indicates that this type of buckling can never be of importance with metal tubes. In the last analysis such a buckling merely amounts to a change of a component of the twisting moment into bending moment. The resulting deflections could never be as great as the bending deflections which would occur if the whole twisting moment were to be applied as a bending moment. In the case of a long piece of rubber tubing, enormous angles of twist can be obtained. This deformation is not especially apparent, as it leaves the tube cylindrical as before; if, now, some of this twisting deformation suddenly goes into bending deformation, the resulting deformation is very spectacular, even if the angles of bending are only a small part of the previous angles of twist. In the case of the steel tube shown in figure 10, which is about as extreme as any practical case could be, the torque at which buckling occurred would only have caused a deflection of 1 inch in the middle of the 53-inch span, if it had all been applied as a bending moment. It is evident that the occurrence of a fraction of this deflection due to a spiral deformation would not even be noticeable.

Returning to the cases where $n>1$, the shape of buckling deflection can be found as follows: From the values of a, b, and c which have been determined, the values of λ_1, λ_2, λ_3, λ_4 are found from (23). Putting these in any three of the four equations of (18), we solve these equations simultaneously for W_2, W_3, and W_4 in terms of W_1. Using these values, the value of n (obtained as elsewhere discussed) and (16), in (13), we obtain the desired expressions for u, v, and w. These expressions contain an indeterminate factor W_1, which is to be expected, as the absolute magnitude of the displacement is indeterminate. These calculations can be made from the results obtained later for short tubes, as well as from the results already obtained for long tubes. However, as the work of solving equations (18) simultaneously is quite laborious, it has been carried out for only one case, that of long clamped edge tubes; the result should apply with sufficient accuracy to most of the experiments and to most practical applications. Using the values of b, c, and a from the fourth line of table II, we find, for long clamped edge tubes

$$\begin{aligned}
w=W_1\Big[&\cos\Big(n\frac{s}{r}+11.54\frac{x}{l}\Big)+1.301\cos\Big(n\frac{s}{r}+4.86\frac{x}{l}\Big)\\
&-0.00054\sinh 12.06\frac{x}{l}\sin\Big(n\frac{s}{r}-8.20\frac{x}{l}\Big)\\
&-0.00172\cosh 12.06\frac{x}{l}\cos\Big(\frac{ns}{r}-8.20\frac{x}{l}\Big)\Big]\\
v=-\frac{1}{n}W_1\Big[&\sin\Big(n\frac{s}{r}+11.54\frac{x}{l}\Big)\\
&+1.301\sin\Big(n\frac{s}{r}+4.86\frac{x}{l}\Big)\\
&+0.00054\sinh 12.06\frac{x}{l}\cos\Big(n\frac{s}{r}-8.20\frac{x}{l}\Big)\\
&-0.00172\cosh 12.06\frac{x}{l}\sin\Big(\frac{ns}{r}-8.20\frac{x}{l}\Big)\Big]\\
u=\frac{d}{n^2l}W_1\Big[&5.77\sin\Big(n\frac{s}{r}+11.54\frac{x}{l}\Big)\\
&+3.16\sin\Big(\frac{ns}{r}+4.86\frac{x}{l}\Big)\\
&+0.0082\sinh 12.06\frac{x}{l}\cos\Big(\frac{ns}{r}-8.20\frac{x}{l}\Big)\\
&+0.0103\cosh 12.06\frac{x}{l}\sin\Big(\frac{ns}{r}-8.20\frac{x}{l}\Big)\Big]
\end{aligned}\qquad(31)$$

where n is given by figure 2 or equation (29).

The results found so far were obtained from (25) and are not accurate for short tubes. To obtain a solution from (24) and (26) is much more difficult. Particular solutions were found as follows: Values of b and c are assumed, and the value of a found from (26). The value of k is then found from an equation obtained by dividing the third by the first equation of (24); H' is now found from the first and then A from the second equation of (24).

The value of H is now computed from (21). This requires the selection of a weighted average value for λ_m^2. For this purpose three solutions for the shape of

the buckling deflection are available, the one above for the case $l/d = \infty$ (clamped edges), and solutions for the case $l/d = 0$ for both edge conditions, given by Southwell and Skan (reference 6). In all these solutions the first two terms involve λ_1 and λ_2, respectively, and the last two terms involve λ_3 and λ_4. These last two terms are much smaller than the first two. In figure 17 the

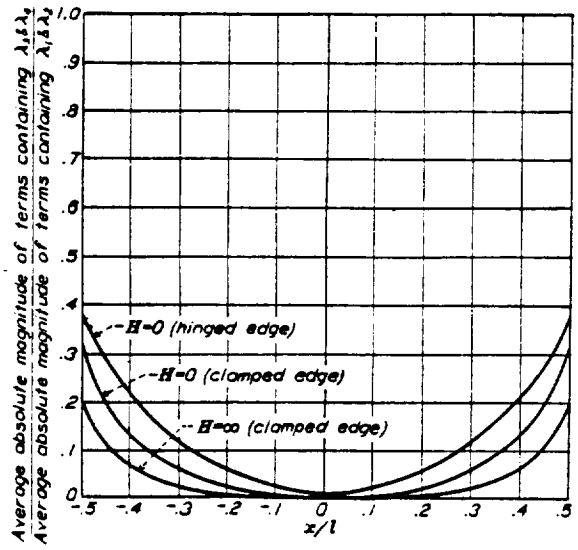

FIGURE 17.—Chart showing relative unimportance of λ_3 and λ_4.

ratio of the average absolute magnitudes of the last two terms, to the average absolute magnitudes of the first two, is plotted against x/l. It will be seen that the last two terms are very unimportant compared to the first two, and hence λ_3 and λ_4 are unimportant compared to λ_1 and λ_2. Comparison of the terms containing λ_1 and λ_2 shows that these are of the same order of magnitude for all of these extreme cases. Equation (21) was therefore taken as

$$H = H'\left(1+\frac{\lambda_1^2+\lambda_2^2}{2k^2}\right) = H'\left(1+\frac{a^2+b^2}{k^2}\right)$$

This is of course rather a rough correction, but it may be considered to be applied, not to the whole solution for A or S, but to the error in the first approximation, as previously discussed.

We now have corresponding values of A and H, satisfying the equations of equilibrium and the boundary conditions. However, the original choice of b and c was purely guesswork, and with different values of b and c we may obtain higher or lower values of A, and therefore of S, for the same value of H. For these higher or lower values of S there will correspond certain values of k and therefore of n. We know that the actual value of n will be that giving the lowest value of S consistent with equilibrium and boundary conditions. It is therefore clear that the smallest values we can find for A in terms of H by the above process will be the correct values.

If we had to try values of b and c blindly, the work would be very difficult, as only a small range of values even result in real values for a, k, A, and H. However, we already know the values of b and c for the extreme cases when $H = 0$ and $H = \infty$, given by Southwell and Skan, and the previous solution obtained from (25). These sets of values of b and c are represented by the points p and q, figure 18. The desired values of b and

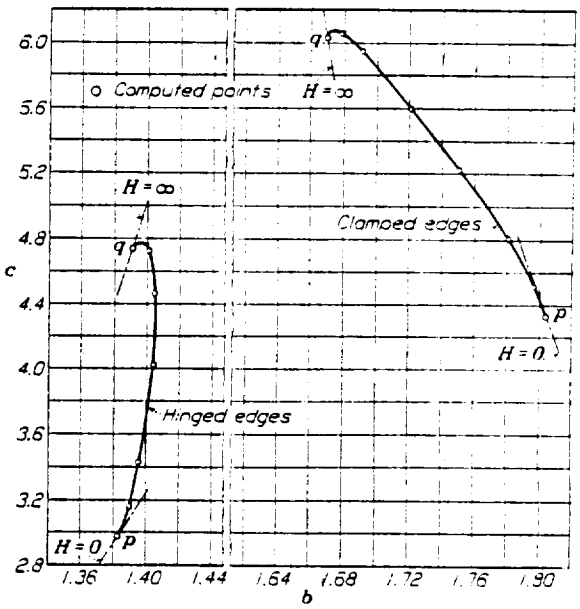

FIGURE 18.—Values found for b and c from $H=0$ to $H=\infty$.

c, for intermediate values of H, are obviously given by points on some line connecting p and q. By trying a number of points distributed over the area between p and q, plotting the results on figure 1, and making use of cross plotting, we locate with sufficient accuracy the lines shown in figure 18, which correspond to the lower part of the curves in figure 1. Points on either side of the lines in figure 18 give points above the curves in figure 1. Table III gives sets of values of b, c, a, k, H', H, and A obtained in this way. Equations (1) are merely formulas which have been found nearly to check the relation between A and H given by these values, as will be seen from the last column of table III. Corresponding values of k and H have been plotted in figure 3, forming the left-hand end of the curves shown, which approach asymptotically the portions previously found, at the right.

The theoretical value of the angle which the buckling waves make with the axial direction is $\tan^{-1}\frac{\lambda_m d}{nl}$ for each of the four components of the wave, as has been pointed out previously. As it has been shown that the components involving λ_3 and λ_4 are comparatively unimportant, and that the other two components are of nearly the same magnitude, an approximate value for the angle of the resultant wave is evidently

$$\theta = \tan^{-1}\frac{\lambda_1+\lambda_2}{2}\frac{d}{nl} = \tan^{-1}\frac{ad}{nl} = \tan^{-1}\frac{a}{k} \qquad (32)$$

A more accurate value for three particular cases can be found from the three available solutions for the shape of the buckling deflection. Setting equal to zero the derivative with respect to s of the expression for w, we obtain the equation of the line at the top or bottom of the wave. The desired angle is the tangent of the slope of this line, or $\tan^{-1} ds/dx$. It is found that, for these extreme cases, the angle is nearly constant near the middle of the tube, and checks the value found from (32) within about 10 percent. Hence (32) is probably sufficiently accurate for a check on the tests, especially as it is difficult to get a very accurate value for θ from experiments. The curves of figure 4 were plotted from (32), using values of a, k, and H from table III. Equation (3) is also obtained from (32), using the value of a for $H = \infty$.

The author wishes to acknowledge the valuable suggestions of Dr. Theodor von Kármán for interpreting the application of the simplified equilibrium equations; the help of Messrs. K. W. Donnell and L. Secretan in carrying out the experiments; and several helpful criticisms from Dr. S. Timoshenko.

TABLE I—EXPERIMENTAL DATA

STEEL TUBES

d	l	$t\times10^3$	$E\times10^{-6}$	Ultimate torque	n	θ
Inches	*Inches*	*Inches*	*Lb./in.²*	*In.-lb.*		°
27.0	86.8	11.5	28.9	12,800	3.5	8
5.98	.469	1.93	31.3	960	44	------
5.88	.375	1.93	31.3	1,020	46	------
5.88	.290	1.93	31.3	1,400	50	------
.319	4.53	1.92	31.3	5.20	2	------
.319	7.81	1.92	31.3	3.39	2	------
.319	12.4	1.92	31.3	3.81	2	------
.319	13.1	1.92	31.3	3.41	2	------
.319	15.8	1.90	31.3	3.19	2	------
.319	21.4	1.99	31.3	3.01	2	------
.319	29.5	1.92	31.3	3.27	2	------
.319	53.5	1.92	31.3	3.20	2	------
5.67	6.0	2.92	31.3	286	13.9	11
5.67	6.0	2.80	31.3	268	13.4	11
3.75	6.0	2.88	31.3	202	10.4	10
3.75	6.0	2.88	31.3	218	11.1	10
1.98	6.0	2.92	31.3	98	6.7	10
5.67	6.0	2.17	31.3	162	15.4	9
5.67	6.0	2.17	31.3	146	13.1	11
3.75	6.0	2.13	31.3	84	10	10
3.75	6.0	2.13	31.3	106	12.5	10
1.98	6.0	2.05	31.3	48	6.6	11
5.67	12.0	2.68	31.3	206	7	9
3.75	12.0	2.80	31.3	128	8	9
1.98	12.0	2.80	31.3	64	5.1	9
5.67	12.0	2.05	31.3	90	10	8
3.75	12.0	2.01	31.3	80	7.9	9
1.98	12.0	2.01	31.3	32	5	7
1.88	24.0	2.34	31.3	48	4	12
1.98	30.0	2.01	31.3	20	4.7	6

BRASS TUBES

d	l	$t\times10^3$	$E\times10^{-6}$	Ultimate torque	n	θ
Inches	*Inches*	*Inches*	*Lb./in.²*	*In.-lb.*		°
5.67	6.0	5.87	16.3	912	11	15
5.67	6.0	5.98	16.3	1,048	11	17
3.75	6.0	6.02	16.3	564	8.8	10
3.75	6.0	5.91	16.3	638	8.7	9
1.98	6.0	5.87	16.3	262	6	10
5.67	6.0	3.07	15.7	170	7.8	10
5.67	6.0	3.11	15.7	192	8	11
3.75	6.0	3.11	15.7	112	10.5	11
1.98	6.0	2.99	15.7	60	7.1	10
1.98	6.0	2.99	15.7	46	7.8	10
5.67	6.0	2.13	15.7	72	15	11
5.67	6.0	2.09	15.7	70	14	13
3.75	6.0	2.09	15.7	50	11.6	11
3.75	6.0	2.13	15.7	46	12.5	12
5.69	12.0	5.96	16.3	764	8.9	9
5.69	12.0	5.90	16.3	776	9	12
5.69	12.0	5.90	16.3	710	10	12
3.75	12.0	5.96	16.3	478	6.7	11
1.88	12.0	5.87	16.3	192	4	9
5.67	12.0	2.09	15.7	44	10	10
3.75	12.0	2.05	15.7	38	9	9
5.67	30.0	5.98	16.3	454	7.2	9
3.75	30.0	5.91	16.3	288	5	9
1.98	30.0	5.98	16.3	126	3	3

GUGGENHEIM AERONAUTICAL LABORATORY,
CALIFORNIA INSTITUTE OF TECHNOLOGY,
MAY 5, 1933.

TABLE II

b	c	a	n^4J^1	n^4BJ	Expression (27)	BJ^1
CLAMPED EDGES						
$7\pi/12$	3.18	1.83	0	24.7	----------	∞
1.780	3.56	2.18	82.2	34.6	33.8	2.19
1.728	4.25	2.75	348.3	57.7	57.7	1.49
1.669	6.03	4.10	2,236	160.6	160.5	1.293
1.641	8.13	5.62	8,442	387	386	1.36
1.623	10.54	7.36	25,620	930	942	1.47
1.606	15.47	10.89	124,500	2,633	2,645	1.72
1.586	30.40	21.50	1,912,500	20,000	20,062	2.37
$\pi/2$	∞	∞	∞	$.385(n^4J^1)^{\frac{1}{2}}$	$.385(n^4J^1)^{\frac{1}{2}}$	∞
HINGED EDGES						
$5\pi/12$	2.27	1.31	0	9.04	----------	∞
1.342	3.33	2.16	135	27.8	28.1	1.39
1.391	4.74	3.21	822	78.3	78.2	1.182
1.414	5.57	3.81	1,707	125.7	125.4	1.20
1.449	7.44	5.17	6,046	297	297	1.29
1.500	14.0	9.82	82,240	1,936	1,945	1.64
1.530	24.9	17.60	861,000	11,000	11,050	2.15
$\pi/2$	∞	∞	∞	$.385(n^4J^1)^{\frac{1}{2}}$	$.385(n^4J^1)^{\frac{1}{2}}$	∞

TABLE III

b	c	a	k	H'	H	A	Rt. side eq. (1)
CLAMPED EDGES							
1.804	4.334	1.977	1.96	----------	0	7.39	7.39
1.796	4.52	2.03	2.18	.67	1.69	7.73	7.98
1.781	4.81	2.14	2.71	2.58	5.30	9.47	9.38
1.751	5.22	2.47	4.10	13.0	20.1	17.04	17.20
1.721	5.59	2.91	6.21	53.6	66.5	36.3	35.9
1.691	5.96	3.53	10.92	377	426	126	126
1.678	6.06	3.86	17.6	2,180	2,300	440	435
1.669	6.03	4.10	$2.62H^{\frac{1}{4}}$	∞	∞	$1.293H^{\frac{1}{2}}$	$1.293H^{\frac{1}{2}}$
HINGED EDGES							
1.393	2.977	1.445	1.18	----------	0	4.40	4.40
1.390	3.16	1.53	1.73	1.52	3.69	6.22	6.33
1.395	3.43	1.70	2.61	6.07	10.38	10.06	9.82
1.404	4.06	2.15	4.63	33.1	43.6	23.3	22.9
1.404	4.46	2.56	7.11	131	153	55.3	54.2
1.410	4.72	2.94	11.6	726	783	180	178
1.391	4.74	3.21	$2.31H^{\frac{1}{4}}$	∞	∞	$1.182H^{\frac{1}{2}}$	$1.182H^{\frac{1}{2}}$

REFERENCES

1. Lundquist, Eugene E.: Strength Tests on Thin-Walled Duralumin Cylinders in Torsion. N.A.C.A., T.N. No. 427, 1932.
2. Bollenrath, F.: Wrinkling Phenomena of Thin Flat Plates Subjected to Shear Stresses. N.A.C.A., T.M. No. 601, 1931.
3. Gough, H. J. and Cox, H. L.: Some Tests on the Stability of Thin Strip Material under Shearing Forces in the Plane of the Strip. Proc. Roy. Soc. London, vol. 137 A, 1932, p. 145.
4. Southwell, R. V.: On the Analysis of Experimental Observations in Problems of Elastic Stability. Proc. Roy. Soc. London, vol. 135 A, 1932, p. 601.
5. Schwerin, E.: Torsional Stability of Thin-Walled Tubes. Proc. of the First International Congress for Applied Mechanics at Delft, 1924, pp. 255–65.
6. Southwell, R. V. and Skan, Sylvia W.: On the Stability under Shearing Forces of a Flat Elastic Strip. Proc. Roy. Soc. London, vol. 105 A, 1924, p. 582.
7. Sezawa, Katsutada and Kubo, Kei: The Buckling of a Cylindrical Shell under Torsion. Aero. Research Inst., Tokyo Imperial Univ., Report No. 76, vol. VI, no. 10, 1931.
8. Donnell, L. H.: The Problem of Elastic Stability. Transactions of The Am. Soc. of Mech. Eng., Aeronautical Division, 1933.
9. Love, A. E. H.: Mathematical Theory of Elasticity. Fourth edition. Cambridge University Press, 1927, p. 532.
10. Greenhill, A. G.: On the Strength of Shafting when Exposed Both to Torsion and to End Thrust. Proc. Inst. of Mech. Eng., London, 1883, P. 182.
11. von Sanden, K., and Tolke, F.: Stability Problems of Thin Cylindrical Shells. Ingenieur-Archiv, Vol. 3, 1932, P. 24.

U. S. GOVERNMENT PRINTING OFFICE: 1933